Volume 117 • Issue 1897
January 2011 • £4.60

www.electronicsworld.co.uk

ELECTRONICS WORLD

THE ESSENTIAL ELECTRONICS ENGINEERING MAGAZINE

- **EXPLOSIVE** END OF ELECTRIC CHARGE AS WE KNOW IT
- **NEW** ON THE ROAD
- **NEW** USB DESIGN PROJECTS

THEORY AND R&D

SPECIAL REPORT

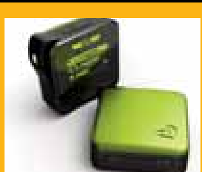

TECHNOLOGY
MOBILE HEALTH ADVANCES

AUDIO
REVOLUTIONARY 3D FILTER

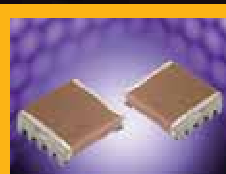

PRODUCTS
SYSTEMS FOR VARIED NEEDS

ALSO IN THIS ISSUE: THE TROUBLE WITH RF: "NO ANTENNA CABLE?"

36

30

44

REGULARS

05 **TREND**
RETAILERS FACE SHORTAGE OF ELECTRICAL GOODS THIS CHRISTMAS

06 **TECHNOLOGY**

08 **ELECTRONICA 2010 REVIEW**

14 **AUDIO COLUMN**
THE WHITE CATHODE FOLLOWER CF
by **Burkhard Vogel**

16 **THE TROUBLE WITH RF...**
NO ANTENNA CABLE?
by **Myk Dormer**

18 **NEW ON THE ROAD**
WIRED FOR SPEED – THE NEW FACE OF THE ELECTRONICS SALESMAN
by **Huw Muncer**

39 **AVIONICS & DEFENCE ELECTRONICS EUROPE 2011 PREVIEW**

44 **NEW USB DESIGN PROJECTS**
USB CONVERSION OF SERIAL AND PARALLEL DEVICES
by **John Hyde**

46 **PRODUCTS**

50 **LAST NOTE**

Cover supplied by FARNELL
More about element 14 on pages 12-13

FEATURES

20 **EXPLOSIVE** THE END OF ELECTRIC CHARGE AND ELECTRIC CURRENT AS WE KNOW THEM – PART 1
Ivor Catt presents a two-part article on the matters of electrical charge and current

26 TRANSMISSION LINE TRANSIENTS
Ian Darney answers the question of '*When a voltage step travels down a transmission line at the speed of light guided by two conductors, where does the negative charge come from on the bottom conductor to terminate the electric field between the conductors*'

30 SMART EXPERIMENTAL MANAGEMENT SYSTEM FOR ELECTRICAL AND ELECTRONIC ENGINEERING LABORATORIES
N. Suha Bayindir, Ilker Degirmencioglu and **H. Ozgur Bayindir** present a Smart Experimental Management System (SEMS) as a compact intelligent laboratory control system

36 REVOLUTIONARY 3D FILTER FOR AUDIO, SATELLITES, CARS, MEDICAL DEVICES & INDUSTRIAL MEASUREMENT
Clemens Par explains how a mathematical filter, named VoiCode, makes the unachievable in professional audio very easy

40 LCD TELEVISION DEMYSTIFIED – PART 1
Fawzi Ibrahim explores the modular structure of LCD receivers, identifying the individual boards and explaining their functions

Electronics World is published monthly by
Saint John Patrick Publishers Ltd,
6 Laurence Pountney Hill, London, EC4R 0BL.

RETAILERS FACE SHORTAGE OF ELECTRICAL GOODS THIS CHRISTMAS

Retailers are facing the prospect of a shortage of the most wanted electrical consumer goods,

such as games consoles and flat screen TVs, as we enter retail's busiest time of the year, warns BravoSolution, a supply management information and solution company.

In a period of ongoing economic uncertainty, companies are continuing to hold on to their cash reserves wherever possible. As such, many suppliers have begun to reduce inventory levels with fears that redundant stock risks significant losses if left unsold. As a result, lead times for electrical components have increased dramatically, hitting dangerously high levels that now stand at an alarming 52 days – five times higher than the previous 10-12 day standard. With Christmas upon our doorsteps, this is a huge concern for retailers, who now risk being left short of supply of some of the most popular electrical products.

According to BravoSolution's analysis, electrical components such as transistors have been affected most in this aggressive inventory dwindle, risking a serious shortage of the most desired consumer electronics, such as games consoles and televisions, and small appliances, including microwaves and food processors, this festive season.

"As consumers, we use the Christmas period as an excuse to spend our hard-earned-cash – whether that is splashing out on a new TV to watch our favourite Christmas specials or treating loved ones to a games console to enjoy on Boxing Day. If inventories continue to remain at dangerously low levels, there is a huge risk that many shelves could remain empty well into the New Year and beyond," said Paul Martyn, Vice President of Global Marketing at BravoSolution. "With lead times for core electrical products hitting unprecedented levels over recent months, there is a real risk that many of the most wanted goods will simply not be available this Christmas."

"Due to the surge in demand, the festive season is always a challenging time for retailers. With sales at risk at such a crucial time of the year, there is a real danger that quarterly results will be affected, which will ultimately have a substantial impact on the profitability and share price performance of both manufacturers and retailers alike."

Top Five Potential Product Shortages:

1. Games consoles
2. MP3 players
3. Televisions
4. DVD players
5. Microwaves

BravoSolution is an international provider of Supply Management Excellence, delivered through software, professional services and category expertise, with a mission to generate value by supporting its clients in the improvement of procurement processes. ***www.bravosolution.com***

"IF INVENTORIES CONTINUE TO REMAIN AT DANGEROUSLY LOW LEVELS, THERE IS A HUGE RISK THAT MANY SHELVES COULD REMAIN EMPTY WELL INTO THE NEW YEAR AND BEYOND"

EDITOR: **Svetlana Josifovska**
Email: svetlanaj@stjohnpatrick.com
PRODUCTION MANAGER: **Tania King**
Email: taniak@stjohnpatrick.com
DISPLAY SALES: **John Steward**
Tel: +44 (0) 20 7933 8974
Email: johns@stjohnpatrick.com
PUBLISHER: **Wayne Darroch**

SUBSCRIPTIONS:
Saint John Patrick Publishers
PO Box 6009, Thatcham,
Berkshire, RG19 4QB
Tel: 01635 879361 Fax: 01635 868594
Email: electronicsworld@circdata.com
SUBSCRIPTION RATES:
1 year: £46 (UK); £67.50 (worldwide)

MISSING ISSUES:
Email: electronicsworld@circdata.com
NEWSTRADE:
Distributed by Seymour Distribution Ltd,
2 East Poultry Avenue, London, EC1A 9PT
Tel: +44 (0) 20 7429 4000
PRINTER: **Pensord Printers**
ISSN: **1365-4675**

St John Patrick Publishers

MEASURING THE ELECTRICAL PROPERTIES OF NANO-CRYSTALS

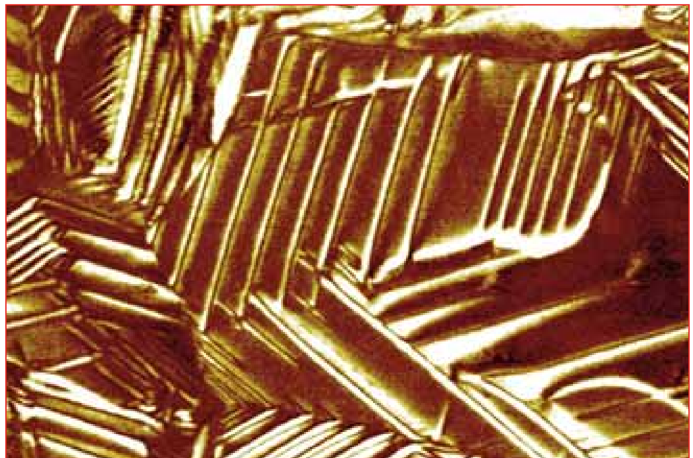

NPL's technique is used to obtain data on the domain-resolved effective single crystal piezoelectric response of individual crystallites in $Pb(Zr_{0.4}Ti_{0.6})O_3$ ceramics

The UK's National Physical Laboratory (NPL) researchers have discovered that by combining textural analysis, through electron backscatter diffraction (EBSD), with piezoresponse force microscopy, quantitative measurements of the piezoelectric properties can be made at a scale of 25nm, smaller than the domain size – that is the electrical features that dictate the material's properties. This is expected to provide more reliable measurement of the electrical properties of materials used in nanotechnology – which could lead to much more accurate devices in the future.

The technique is used to obtain data on the domain-resolved effective single crystal piezoelectric response of individual crystallites in $Pb(Zr_{0.4}Ti_{0.6})O_3$ ceramics. The results offer insight into the science of domain engineering and provide practical information for the future development of new nano-structured ferroelectric materials for memory, nano-actuators and sensors.

"As the drive to miniaturise devices continues we will need to make changes in how they are made to increase performance levels, so measuring how electrical materials behave on the nanoscale is essential," said Tim Burnett from NPL. "The problem with making things that are nano-sized is that it is very difficult to measure their performance. Our research at NPL will enable genuine comparisons to be made and promote a better understanding of the nanotechnology of electrical materials and devices."

Scanning probe microscopy (SPM) won the Nobel Prize in 1986. It uses a nano-sized probe to feel the surface of a material – akin to a finger reading Braille on an extremely small scale. The technique can also measure the electrical properties of materials used in nanotechnology – and "feel" how the material reacts when electricity is passed through it.

Mobile Health Device Links Patients and Healthcare Professionals

UK-based technology product design and development firm Cambridge Consultants announced a new product concept based on its Continua-compliant Vena platform. The Minder, powered by Vena, enables continuous, real-time medical data collection and transmission via cellular networks. Increasing the accuracy and frequency of patient data reporting, the Minder demonstrates a new technology solution that can lower the cost of healthcare by improving the quality of patient care.

Doubling as a pocket-sized digital patient checklist, Minder captures wireless medical data and transmits it to a patient's online health record, creating higher volume and higher quality data for Electronic Medical Records (EMR). Moreover, Minder can receive real-time updates to the checklist, thereby allowing two-way communications with healthcare professionals or caregivers, enabling more meaningful use of e-health records.

Usually, a hospital visit is required in order to record data, such as ECG or blood pressure readings, into a patient's EMR. However, as wireless-enabled medical devices continue to grow in number, the novel Minder device showcases a viable pathway for such readings to be acquired and transmitted remotely. For physicians and hospitals, this would provide access to more accurate data to work with, while increasing efficiency and decreasing unnecessary and expensive hospital visits.

Direct comms links between doctors and patients promote independence, especially among the elderly

The Vena platform

The Vena technology used in Minder, leverages Cambridge Consultants's experience with CSR's BlueCore and Qualcomm's Wearable Mobile Device (WMD) hardware and implements Continua Health Alliance standards for Personal Area Network (PAN) and Wide Area Network (WAN) interfaces. Devices based on Vena can receive data via Bluetooth or USB from any Continua Certified devices and transmit this data via HL7 over cellular networks, thus empowering users to manage health and wellness anytime, anywhere.

The Vena wireless healthcare software stack, embeds the Bluetooth Health Device Profile (HDP) optimised for the secure transport of medical data and the IEEE 11073 standards for compatible exchange of information between devices.

REVOLUTIONARY HEAT TRANSFER MATERIAL LAUNCHED

Elektron Ventures has unveiled a brand new porous copper material that will transform cooling systems and enable faster processing clock speeds.

AdvarienCu – a pioneering copper foam created using a patented process – is materials efficient, non toxic and highly cost-effective.

Tests by a leading academic research group found AdvarienCu-based liquid cooling devices to be three to ten times more effective at transferring heat into a passing coolant than a microchannel water block of similar size.

The innovative open cell copper foam allows significant controllable porosity from 50-85%, resulting in a vast specific surface area, making AdvarienCu an extremely effective material for exchanging heat into a passing cooling fluid. The benefits of copper for thermal management are well recognised, however AdvarienCu's open cell porous structure allows coolant fluid to carry heat away to a radiator more effectively than expensive micro-machined structures and removes the need to install a bulky fan.

"AdvarienCu is a new and exciting material for the liquid cooling of semiconductor devices which offers users dramatic technical and commercial benefits. It is a simple, cost-effective manufacturing process and it is ideal for use in PCs, servers, supercomputers, games consoles and industrial power conditioning equipment," said Neill Ricketts, managing director of Elektron Ventures.

AdvarienCu can be fused at an atomic level to a base plate, which coupled with its unprecedented surface area, ensures ground-breaking levels of heat transfer between device and cooling fluid. The process, known as Lost Carbonate Sintering (LCS) was developed by the University of Liverpool and has a world-wide patent in place.

■ EnSilica and Pebble Bay are collaborating to target the automotive electronics design market by porting ERIKA Enterprise, the free-of-charge, open source RTOS for automotive systems, to EnSilica's family of highly configurable and low-power eSi-RISC soft processor cores.

The ERIKA Enterprise RTOS is an open-source implementation of the ISO 17356 API that has been specifically developed for use in automotive applications, providing a minimal 1-4KB Flash real-time kernel and implementing an open source version of the OSEK/VDX open architecture specification for automotive electronics systems. It supports both single and multi-core embedded systems.

■ Iberdrola and ERDF have decided to join efforts towards an open PLC (Power Line Communications) standard that will bring interoperability to smart metering. To accomplish this, Iberdrola will assemble a team of experts to define a common PLC telecommunications profile. The resulting effort will take into account the strengths of each protocol already being used by each company. The updated single set of telecommunications requirements will guarantee interoperability among systems and devices produced by different manufacturers. Technical specifications are to be open and public, as both utilities share the same vision on PLC architectures based on truly open standards.

MATHWORKS ANNOUNCES RELEASE 2010B OF THE MATLAB AND SIMULINK PRODUCT FAMILIES

At Electronica this year MathWorks discussed the recently announced Release 2010b (R2010b) of its MATLAB and Simulink product families. Among the expanded set of tools and features in this release are new communications system design capabilities; automated PID controls tuning; GigE Vision hardware standard support and enhanced Simulink and Stateflow support for creating reusable models.

R2010b also introduces SimRF, which adds system-level modelling of RF receiver architectures. This release updates 84 MathWorks products, including Polyspace code verification products.

"There are new capabilities in MATLAB and Simulink for Multidomain Signal Processing Systems," said Graham Reith, Senior Application Engineer for Signal Processing and Communications at MathWorks. "These cover system and algorithm design, help with FPGA design automation and Embedded C code generation."

Updates to MATLAB that support advanced programming include custom enumerated data types, 64-bit integer arithmetic and a number of enhancements to the development environment.

Other MATLAB family highlights in R2010b include Parallel Computing Toolbox – GPU support of CUDA-enabled NVIDIA hardware for accelerated computation; Control System Toolbox, consisting of new commands and graphical tools for modelling and automatically tuning PID controllers; Image Acquisition Toolbox, which uses a plug-and-play camera input based on the GigE Vision hardware standard and Communications Blockset: New System objects for communications system design in MATLAB among others.

With R2010b, Simulink offers a new signal type and subsystem enhancements that help reduce block counts, simulation time and memory usage for large models.

Analog Devices Advances Ultrasound System Design With Low-Power Receiver ICs

ADI's new, fourth generation of its octal (eight-channel) ultrasound receivers, was discussed at Electronica this year with the introduction of two new ICs that reduce system size, complexity and power consumption for high-end, mid-range and portable ultrasound systems.

The need for smaller, faster, lower-power ultrasound equipment continues to grow as hospitals, medical clinics and medical emergency units increasingly rely on more sophisticated ultrasound equipment for providing diagnostic imaging. InMedica, the medical research division of IMS Research, predicts worldwide ultrasound revenues will grow from $4.9bn in 2009 to more than $6bn by 2012.

The new ADI octal ultrasound receivers help system designers manage the design challenges in getting the best image quality at lowest power for high-end and portable systems

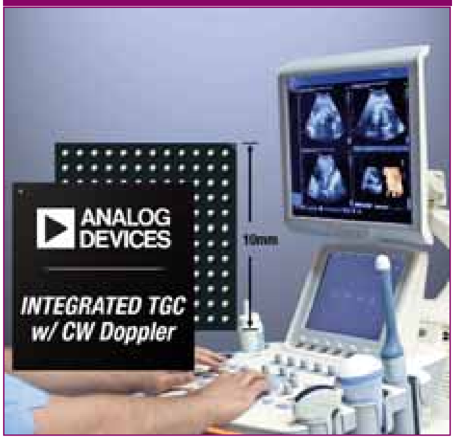

The new AD9278 and AD9279 receiver chips each integrate ADI's world-leading data conversion technology for low noise TGC (time-gain-control) mode performance while providing high dynamic range I/Q demodulators that reduce the power and area for implementation of CW (continuous wave) Doppler processing. The new octal ultrasound receivers provide the highest available output-referred large-signal SNR – up to 67 dB – enabling improved sensitivity in diagnostic ultrasound systems while reducing board space up to 40%.

"Ultrasound equipment designers must continually balance new and changing demands for higher image quality and increased power efficiency," said Patrick O'Doherty, vice president for the Healthcare Group at Analog Devices. "The new AD9278 and AD9279 octal ultrasound receivers help system designers manage the design challenges inherent in trying to get the best image quality at the lowest power for either high-end or portable systems."

TMS320C66X DSP DELIVERS INDUSTRY'S TOP RESULTS ON FIXED AND FLOATING-POINT PERFORMANCE

At the Electronica event this year, Texas Instruments (TI) disclosed that its new TMS320C66x digital signal processor (DSP) generation surpasses the performance of any other DSP core in the industry, achieving the highest scores on both fixed- and floating-point performance according to benchmark studies conducted by the independent third-party analysis firm, Berkeley Design Technology (BDTI).

Testing the C66x DSP core separately on the fixed-point performance and the floating-point categories of the BDTI DSP Kernel Benchmarks suite yielded the highest scores in the industry for both sets of tests. The score for the C66x DSP core on the floating-point category of the benchmark is more than two times higher than any previously benchmarked device.

"On floating-point performance the C66x delivered a BDTImark2000 (score of 10,720) – far above the performance of previous-generation floating-point DSPs," BTDI explained in its InsideDSP newsletter. "This will enable developers to create initial application implementations using floating-point math and then decide whether performance-intensive sections of the code should be migrated to fixed-point to boost performance [and] having both on the same chip should prove to be a real advantage."

As a combined fixed-and floating-point DSP core capable of instruction by instruction execution of the two processing modes, TI's C66x core achieves even greater performance in an application where each segment of code is executed in its native processing mode. Integration of fixed-and floating-point capability in the C66x DSP core eliminates costly algorithm conversion from floating-point to fixed-point and allows developers to create code with high precision that runs on a high-performance device.

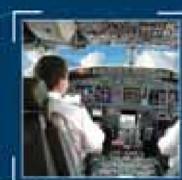

Renesas Unveils a New Control IC for Automotive Applications

Many companies launched a variety of devices for automotive applciations during the Electronica event this year, and Renesas Electronics is also one of them. The supplier of advanced semiconductor solutions announced the availability of its new control IC (part number μPD168891) for automotive light emitting diode (LED) headlights.

The main features of the μPD168891 IC include an integrated current-control function for constant-current drive of LEDs; integrated protection functions essential for automotive applications, including LED current and external MOSFET overcurrent protection; and a newly developed compact package with low thermal resistance. The new device can be combined with other devices, such as MOSFETs, Schottky diodes and choke coils, to build electronic-control units for driving LED headlights, such as automotive headlights.

The μPD168891 device can provide constant-current drive control for up to 12 power LEDs connected in a series. The voltage boost switching frequency can be set to a maximum of 500kHz, a rate slightly lower than the AM radio frequency band, to prevent interference with the car audio system.

Renesas launched a whole range of solutions for automotive applications

Samples of the μPD168891 control IC are available now; volume production is scheduled for the first half of FY2010.

NEW PCI EXPRESS ROOT COMPLEX LITE SOLUTION USES THE LATTICE ECP3 FPGA FAMILY

Lattice FPGA

At Electronica this year, Lattice Semiconductor showcased the PCI Express Root Complex (RC) Lite solution based on the LatticeECP3 and LatticeECP2M FPGA families for use in simple bridging application to any legacy host bus.

Using a low-cost programmable FPGA platform, designers can implement the specific bridge function that matches the interface available on their particular host CPU. The solution also allows designers the flexibility to implement multiple bridges or different configurations of bridges in a single FPGA, reducing the number of components on the board.

"An FPGA-based PCI Express RC Lite solution provides system designers with a flexible way to support intelligent bridging functions between today's high-performance ASSPs that support only the serial PCI Express host interface and legacy CPU parallel host interfaces," said Lalit Merani, Lattice Senior Product Marketing Manager. "Users may choose to maintain support for legacy CPUs due to legacy code compatibility, or because the CPU has been qualified for certain markets, such as military, satellite or industrial."

The PCI Express RC Lite IP core provides a x1 or x4 root complex solution from the electrical SERDES interface, physical layer, data link layer and a minimum transaction layer in the PCI Express protocol stack. The PCI Express 1.1 x1 RC Lite IP core requires approximately 4500 FPGA look-up tables (LUTs) in 16-bit mode. The PCI Express 1.1 x4 RC Lite IP core requires approximately 10,500 FPGA LUTs in 64-bit mode.

SILICON SENSING'S NEW PINPOINT MEMS GYRO SHOWN AT ELECTRONICA

At the Electronica event this year, Silicon Sensing showcased its new class of small precision MEMS navigation and pointing gyros created specifically for tight financial, space and power budgets.

At under 6 x 5 x 1.2mm, weighing less than 0.08g and drawing 4.2mA on its 3V supply, the PinPoint gyro provides an excellent rate output stability over time, temperature, vibration and shock, which were met with great approval from various customers.

"There was a tremendously positive reaction from key customers involved in our pre-launch evaluation programme, with several taking production parts for existing products whilst others have selected PinPoint for their next application, " said Eric Whitley, Business Development Executive at Silicon Sensing. "We have now commenced full production and are talking a wide variety of potential customers for whom this gyro offers an excellent solution."

Among Silicon Sensing's customer is Futaba, a Japanese manufacturer of remote control model helicopter electronics and controls, who had chosen PinPoint for its next generation servo-controllers.

"PinPoint is the only MEMS gyro on the market to function using a fully balanced vibrating silicon ring. Other designs all use various forms of simple unbalanced, open-loop vibrating mass structures – like a tuning fork or a comb design. PinPoint's 3mm diameter balanced ring of resonates at 22kHz in a closed-loop control system. This is similar to an infinite number of tuning forks integrated to create a fully balanced vibrating circular structure and offers outstanding, reliable performance," added Whitley.

Silicon Sensing's tiny new MEMS gyro

New technology access, data and discussion – a winning blend for electronic design engineers

Aakriti Kaushik
PR Manager,
Global and Europe
FARNELL

Time pressured electronic design engineers face a range of challenges that often require additional resources and support. The electronics industry has always been a fast moving and innovative sector and in order to stay competitive, engineers need to make sure they understand and utilise the very latest technologies, techniques and components.

Now, more than ever before, there is immense pressure to shorten design cycle times in order to get new products to market as quickly as possible. The fact that design teams are typically smaller with engineers sometimes being tasked with specifying components that are outside of their area of core technical knowledge only serves to make new product design even more challenging.

RESPONDING TO A CHANGING WORLD

Farnell is in close touch with the electronic design engineering community and this has enabled them to recognise industry and technology trends and respond to them with a range of innovative programs and initiatives, all of which are set against a fast and exciting transition to online purchasing, information sharing and discussion. Farnell has led the way in the distribution sector by continually evolving its business model and innovating to meet the needs of its customers.

Breadth of product range and suppliers has and will always be a cornerstone of a distributor's value proposition if it is to present itself as a realistic 'one-stop' portal for design engineers – Farnell offers over 500,000 products from 3,500 suppliers to comprehensively satisfy this pre-requisite. Of course, a wide product range is only of value if it is available; Farnell recognises the importance of this and has logistics systems and procedures in place that give customers the assurance of next day delivery across the range.

NEW PRODUCTS DRIVE INNOVATION

Access to new technologies is essential for designers seeking to advance the functionality and capabilities of their new product designs. Farnell adds over 100 new technologies online every day. These are often from niche suppliers at the forefront of research, development and manufacture of new devices and modules.

The new Technology First product Microsite provides clear and comprehensive information about these new technologies and makes it easy for engineers to select and design-in devices that can give them a crucial competitive edge.

Each week the site selects and showcases six new products with quick, one-click access from the homepage to more detailed information and a useful product brief. Devices from previous weeks are also easily viewed from the homepage. Other key features of the new product Microsite include applications information, online audio training modules, video demonstrations and additional resources such as selection guides, application notes and reference designs.

The new product Microsite links to the element14 online community, the first of its kind, to allow users to find and share additional information, take part in discussions with other engineers and ask questions.

Further initiatives including i-Buy the free online eprocurement solution, eQuotes that provides a streamlined, efficient way of receiving quotes online and a wide range of packaging innovations adds to the overall offering from Farnell. The result is an invaluable resource and true one-stop location that helps design engineers take their projects from initial concepts to market ready, industry-leading products more efficiently and effectively.

ABOUT FARNELL

Farnell is the leading multi-channel, high service distributor of electronic components, electrical parts, industrial and maintenance, repair & operations products, supporting millions of engineers and purchasing professionals throughout Europe and Asia with the latest technologies. Farnell is celebrating 70 years, making a difference in the electronics industry in 2009. Farnell employs over 1200 people in more than 20 countries around the world and trades in over 100. With over 500,000 products in stock from over 3000 suppliers, our product portfolio continues to expand, offering our customers the very latest technologies.

Farnell is the current holder of the prestigious 'Environmental' award which was presented to the company at the 2010 Elektra Awards.

Farnell is part of the global Premier Farnell Group, which works across geographic and business boundaries. Sharing these facilities and best practice Farnell distribute a huge range of electronic components, electrical parts and wholesale electronics.

For more information visit the Farnell website www.farnell.co.uk

The Common Cathode Gain Stage with Active Anode Load CCA

Burkhard Vogel presents a series of short features with general remarks on triodes in audio applications

THE INPUT GAIN stage of Mr John Broskie's Aikido amplifier (Tube Cad Journal, **www.tubecad.com**) triggered me to take up the below given CCA alternatives. Loading the anode of a CCS (V1) with a current source (V2) and changing the cathode load situation of each valve leads to very different gain and output resistance results.

Because of the very much lower distortion creation Mr Broskie recommends to leave the cathode resistors un-bypassed. However, it's interesting to see what happens if we add cathode capacitances C_{c1} and C_{c2} of a value that does not hurt a flat frequency and phase response in B_{20k}. The respective four different gain and output resistance subscript possibilities are given in **Figure 2**.

Driven by the same anode current the general gain equation for a CCA gain stage à la **Figure 1** with two different triodes and un-bypassed cathode resistors becomes:

$$G_{uu}(R_L) = \frac{v_o}{v_i} = -\mu_1 \frac{1}{1+\frac{r_{a1}+(1+\mu_1)R_{c1}}{r_{a2}+(1+\mu_2)R_{c2}} + \left[r_{a1}+(1+\mu_1)R_{c1}\right]R_L^{-1}} \quad (1)$$

Setting $R_{c2} = 0\Omega$ leads to G_{ub}, setting $R_{c1} = 0\Omega$ leads to G_{bu} and setting $R_{c1} = R_{c2} = 0\Omega$ leads to G_{bb}. The same applies to the output resistance R_o equations. The general and un-bypassed case of R_o at the anode of V1 becomes thus:

$$R_{o.uu} = \frac{\left[r_{a1}+(1+\mu_1)R_{c1}\right]\left[r_{a2}+(1+\mu_2)R_{c2}\right]}{r_{a1}+(1+\mu_1)R_{c1}+r_{a2}+(1+\mu_2)R_{c2}} \quad (2)$$

Setting $R_{c2} = 0\Omega$ leads to $R_{o.ub}$, setting $R_{c1} = 0\Omega$ leads to $R_{o.bu}$ and setting $R_{c1} = R_{c2} = 0\Omega$ leads to $R_{o.bb}$.

With $r_a = r_{a1} = r_{a2}$, $\mu = \mu_1 = \mu_2$ and $R_c = R_{c1} = R_{c2}$, the use of a double-triode will make things less complex. The gain stage's very high sensitivity to output loads requires R_L dependent gain equations:

$$G_{uu}(R_L) = -\mu \frac{1}{2+\left[r_a+(1+\mu)R_c\right]R_L^{-1}} \quad (3)$$

$$G_{ub}(R_L) = -\mu \frac{r_a}{2r_a+(1+\mu)R_c+r_a\left[r_a+(1+\mu)R_c\right]R_L^{-1}} \quad (4)$$

$$G_{bu}(R_L) = -\mu \frac{r_a+(1+\mu)R_c}{2r_a+(1+\mu)R_c+r_a\left[r_a+(1+\mu)R_c\right]R_L^{-1}} \quad (5)$$

$$G_{bb}(R_L) = -\mu \frac{1}{2+r_a R_L^{-1}} \quad (6)$$

and as the output resistances of the four versions we obtain:

$$R_{o.uu} = \frac{r_a+(1+\mu)R_c}{2} \quad (7)$$

Figure 1:
CCA circuit

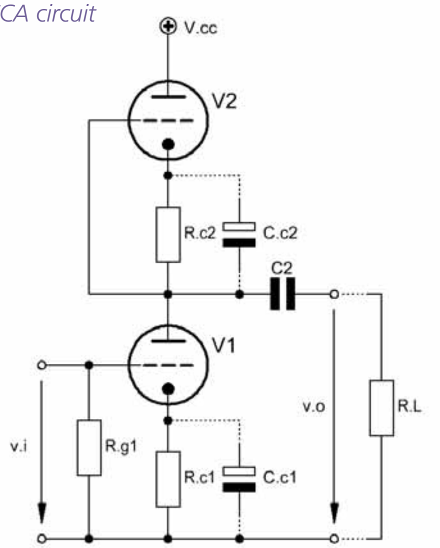

***Figure 2:** Equivalent circuit of Figure 1*

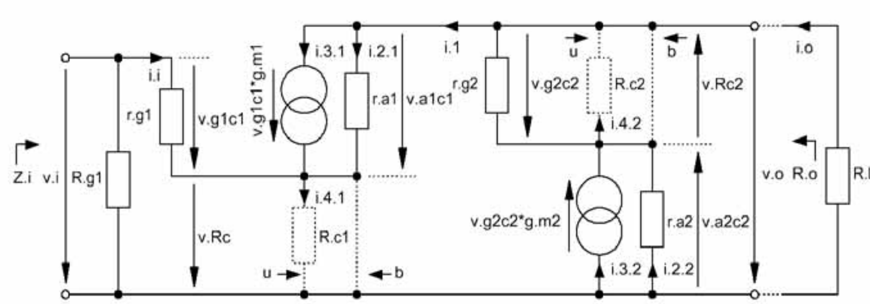

uu = R.c1, R.c2 un-bypassed
ub = R.c1 un-bypassed, R.c2 bypassed
bu = R.c1 bypassed, R.c2 un-bypassed
bb = R.c1, R.c2 bypassed

$$R_{o.ub} = R_{o.bu} = \frac{r_a\left[r_a + (1+\mu)R_c\right]}{2r_a + (1+\mu)R_c} \qquad (8)$$

$$R_{o.bb} = \frac{r_a}{2} \qquad (9)$$

Concentrated on V1 alone concerning the input impedance Z_i and the input capacitance C_i and we can take **Equations 7**, **8** and **9** from Part 2 of this series of articles. However, we have to integrate into these equations the gains from above.

By setting R_L = infinite the calculation of the value of C_{c1} works well with the Equations 2 and 3 from Part 3 of this series. To get the V1 cathode resistance in these equations R_a must be replaced by "$r_a+(1+\mu)R_c$" (= differential resistance of $V2_u$) or by "r_a" (= internal resistance of $V2_b$). Without big error we can calculate C_{c2} = $(2\pi f_c R_{c2})^{-1}$, f_c<<20Hz.

The first three graphs show the most relevant traces of the example double-triode. I've chosen the ECC83/12AX7 at a constant $V_{a1} = V_{a2}$ = 200V because this high-μ triode shows the different results better than a low-μ triode like the 6SN7 (μ ~ 20) (see the last two graphs; "$_k$" indicates the number of the ten I_a values from 0.2mA to 1.6mA).

In contrast to the ECC83, two relevant graphs of the 6SN7 at a constant $V_{a1} = V_{a2}$ = 150V. R_{g1} should be chosen rather low (≤ 50kΩ) because of the relatively high Miller capacitance caused by C_{ga1} = 4pF ("$_k$" indicates the number of the ten I_a values from 0.5mA to 16mA).

Coming in the next issue is *Part 9: 'The μ-Follower'*

If you missed any of the previous parts, you can order them online by going to Electronics World's website at www.electronicsworld.co.uk

Figure 5: *ECC83 CCA output resistances R_o vs. anode current I_a (R_L = 1MΩ))*

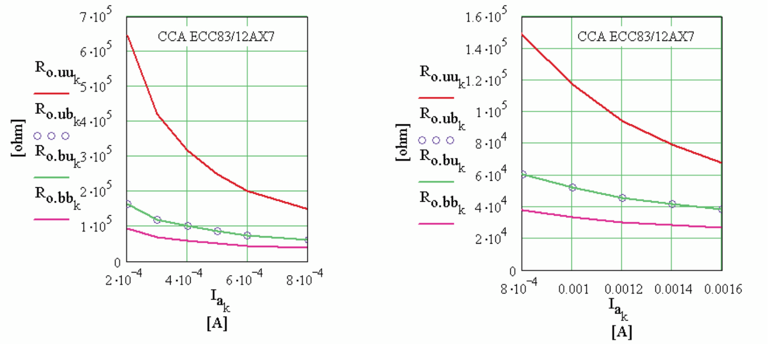

Figure 3: *ECC83 CCA gains G vs. anode current I_a (R_L = 1MΩ)*

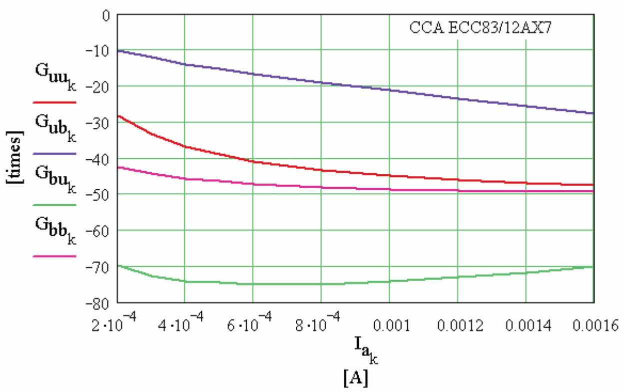

Figure 6: *6SN7 CCA gains vs. anode current I_a (R_L = 500kΩ)*

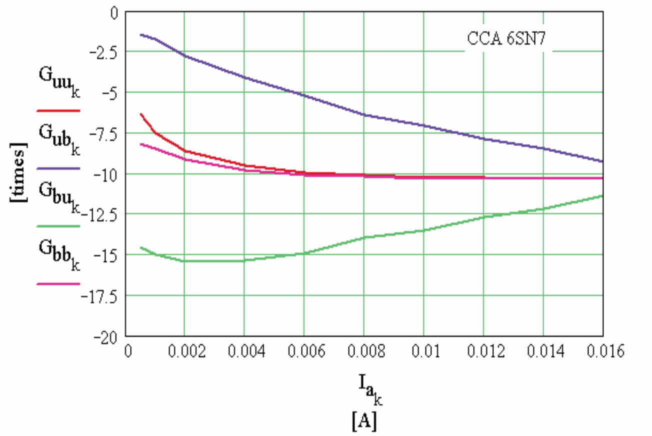

Figure 4: *ECC83 CCA gains G vs. output load R_L (I_a = 1.2mA))*

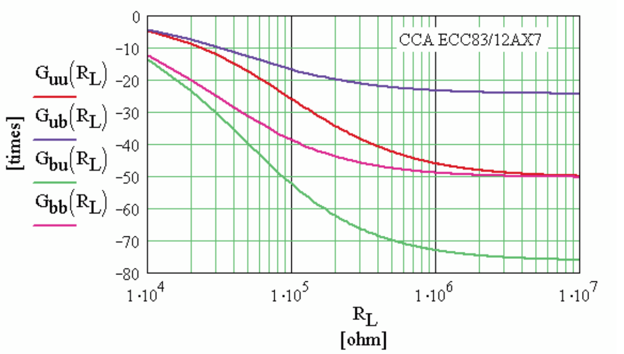

Figure 7: *6SN7 CCA output resistances vs. anode current I_a*

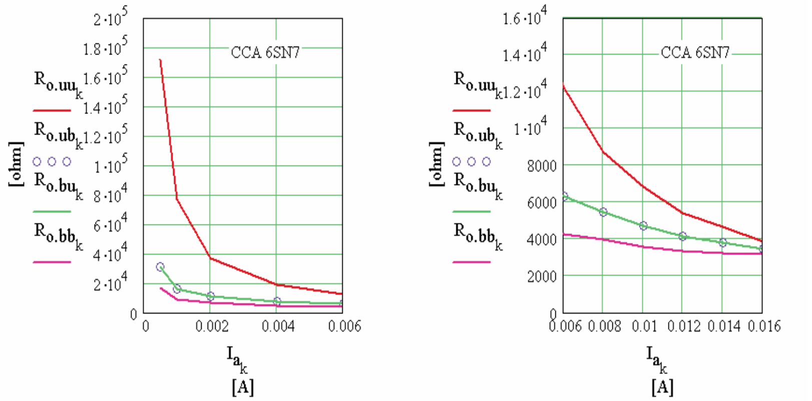

No antenna cable?

Myk Dormer

QUITE FREQUENTLY, in low-power wireless applications, the title of this article is a correct description. There often is 'no antenna cable'. Or rather, the 'cable' is an insignificantly long piece of microstripline connecting the module output pin to an on-board antenna, or to the RF connector that constitutes the electrical and mechanical mount for a co-located proprietary helical or whip. Sometimes the module itself actually includes the antenna (a loop, wire helical or ceramic chip) as well.

This happy state of affairs is not, however, always the case. The antenna cannot always be placed on the target board. Sometimes a short cable is required, such as where a shielded housing requires the antenna to be mounted through its wall or where the radio device is carried in a metal-bodied vehicle. Sometimes the cable is long, as in cases where the antenna is mounted meters, or tens of meters, above the radio installation, to provide enhanced range, to accommodate a larger antenna installation, or to 'see' over an obstacle.

In all these cases, a connection must be made between the radio device and the antenna, and that connection must impose the minimum RF loss, be resistant to pick-up of spurious signals, and present a consistent 50 ohm (in most cases) characteristic impedance. A coaxial cable is (almost) always used, but there are a bewildering variety of 'coaxes' to choose between.

"A CONNECTION MUST BE MADE BETWEEN THE RADIO DEVICE AND THE ANTENNA, AND THAT CONNECTION MUST IMPOSE THE MINIMUM RF LOSS"

Even discounting the obviously unsuitable audio, 75 ohm video and other non-50 ohm data cables, you will see types ranging from 2mm diameter (or thinner) miniature cables, up to the barely flexible, hose-pipe sized examples used for professional high-power transmitters. As far as the low power radio user (who need not be concerned with power handling and voltage flash-over), the reason for this plethora of types is RF loss.

Here are a few common types:

Cable	Diameter	433MHz	869MHz	2.4GHz	(loss)
RG178	1.9mm	0.94dB/m	1.5dB/m		
RG174	2.5mm	0.66dB/m	1.3dB/m	2dB/m	
RG58	5mm	0.35dB/m	0.65dB/m	1.1dB/m	
RG8	10mm	0.14dB/m	0.22dB/m	0.39dB/m	
RG218	22mm	0.08dB/m	0.11dB/m	0.21dB/m	

From the figures in this (admittedly approximate, and drawn from a variety of datasheets) table there seems nothing to worry about: after all, what is a dB here and there?

It's range, efficiency and power consumption. An 869MHz telemetry system with a 5m (only 16 feet) run of RG174 to the antenna has added over 6dB of loss to the link margin calculations. This represents three quarters of the transmitter power being wasted, or looked at another way, the range in free field being more than halved.

Obviously, higher spec cables will reduce this effect (an equal length of RG8 is only 1.1dB) but price is greatly increased (RG8 costs over twice as much as RG174, and specialist low loss RF types cost more again) and the handling, of thicker, less flexible, cables can present serious problems. Despite this, the design rules are clearly obvious:

- Minimise the length wherever and however possible;
- Use the best cable your budget and mechanical constraints permit.

Or consider an alternative: Don't use an RF cable at all. As low-power radio modules tend to be small, it can be practical to mount the entire radio portion of the circuit at the antenna location (in a suitable, environmentally resistant housing), with a much cheaper, less critical multi-core signal/power cable replacing the RF coax. This cable only needs to carry power, baseband signals and control data-streams. A five or six conductor cable will usually be sufficient.

The advantages of this 'active aerial' method are considerable:

- No RF loss problems;
- No RF emission or pick-up from the antenna cable run;
- Inexpensive 'alarm' or 'telephone' type multi-core cable;
- Wireless module is distanced from other interference causing circuits;
- Expensive RF connectors are avoided.

The main challenge in this method is in designing a suitably well-sealed and robust enclosure. My recent tests are pointing towards the use of simple domestic 32mm internal diameter PVC waste pipe to contain both radio and aerial together.

This material provides adequate internal volume to accommodate many types of aerial, wireless modules and support circuits while being inexpensive, robust and easily worked. With luck I shall be testing practical 'active antenna' radios in early 2011. ■

Myk Dormer is Senior RF Design Engineer at Radiometrix Ltd
www.radiometrix.com

WIRED FOR SPEED

the New Face of the Electronics Salesman

Huw Muncer

HUW MUNCER OF TYCO ELECTRONICS'S CIRCUIT PROTECTION BUSINESS UNIT IS ALWAYS ON THE ROAD. AS A SALES MANAGER, HE SEES WHAT ENGINEERS ASK FOR AND NEED, BUT ALSO HOW AN ENGINEER'S JOB HAS CHANGED OVER THE YEARS

"No longer is the salesperson the customer's first line of communication when inquiring about a product"

I HAVE BEEN a salesperson for the electronics industry for more than 20 years. During that time I've observed that not only has the industry itself been turned on its head, but that the manner of selling components has also changed dramatically.

In the past, when embarking on the road to sell electronics components I used to pack my samples and a clean shirt in my car's boot on a Monday morning and, with a quick look at a map, I was off to the first address topping my list. Sometimes my appointments were made by the sales office, but often they were cold calls where I was trying to get a foot in the door. It was a slow process with a lot of time wasted along the way. In contrast, when I make a sales call today, it is only by appointment, that I made myself, and I use sat-nav to get there.

The difference, of course, is that technology has made the sales call a significantly less time-consuming endeavour. No longer is the salesperson the customer's first line of communication when inquiring about a product. Engineers first research their options on the Internet. With all the online databases and websites available, they can begin their search looking for what they think they need before trying to access what they actually require. This has turned the job of a salesperson on its head. We are no longer the key source of initial information for the engineer and the latest printed databook is no longer the hottest commodity we have to offer.

Cold calling still goes on but at a greatly reduced level. The cold call has been mostly replaced by another form of technology: the 'cold email', which also has taken over from the traditional mail-shot. An email cold-call is seen as less invasive because it can be deleted if the customer isn't interested. It can also be helpful for sending preliminary information to customers that can be acted upon later. This way when you call a company you have emailed in advance, there is a chance they will already know a bit about you.

Conversely, email can speed up the follow-up process. Since the life of an email is limited and the timing of e-marketing is crucial, this type of communication must often be followed-up on swiftly.

The speed of reaching the designer with information about a new product has also increased exponentially. It's always been the case that with a new product or application the salesperson must find ways to target sell. In the 'olden days' a new technology was launched and advertised in trade magazines where engineers could use 'bingo cards' to mail in their interest in a promotion. It could take up to three months for this type of sales lead to follow up on. Today it is faster and easier for a potential customer to inquire about a product they have seen in an online database or in an electronic ad or website, but it is much more difficult to catch the attention of an engineer who is presented with so many new forms of advertising. And, unfortunately, any delay in responding to a request means the salesperson is out of the picture.

The actual sales call itself is also much different today. Now when I go on a visit it is very noticeable just how quiet offices have become. People use their computers rather than phones, and engineers seem more reluctant to call in person than they did in the past. In fact, if you get an in-person visit now it usually means there is a potential problem. No longer are engineers sitting at desks with big boards designing by hand as they did ten years ago. Everyone is more mobile, designing on laptops, conducting online meetings or working from home.

So is this the death of the electronics salesman? In the traditional sense the answer is probably yes. But more precisely our roles have changed to accommodate the changing ways of communicating information. One important thing to remember is that companies never put all their product possibilities and limitations on data sheets. This is not because they are trying to be evasive, but because a

"No longer are engineers sitting at desks with big boards designing by hand, as they did ten years ago"

component can be used in so many ways, in many different devices, that it is impossible to address every eventuality on a "piece" of paper – electronic or otherwise. So it is more necessary that a salesperson partner with the design engineer to look into all the finer points of the component that engineers think they want. And the option, when necessary, to communicate face-to-face is also important.

This one-on-one communication is where today's salespeople can demonstrate their real value. By possessing an in-depth knowledge of the product range the salesperson can guide an engineer to just the right component for a very specific technology requirement, which – most importantly – may be the one they already identified or it could be something completely different.

To navigate this new terrain, salespeople must be more than an information source of specs and feeds; we must be true partners to our customers so that we can guide them through a world of possibilities and help them hone in on what is best for their particular design.

Along with partnering more closely with design engineers to help them sort through the myriad products they must evaluate, speed and flexibility are the key attributes of the today's electronics salesperson. The Internet is our most important sales tool. As our company's 'face' to the world it must provide information and also offer a means to communicate.

The use of design forums, portals, online catalogues and blogs has widened an engineer's access to information and their ability to participate and comment on information. This not only helps the company convey information to the engineer, it gives the engineer a broad spectrum of knowledge before they meet with salesperson.

Today, the job of an electronics salesperson's success is completely dependent on his or her ability to deliver information in a timely and relevant way. The job has radically changed from the way it was 20 years ago. And, I think, it has changed for the better. ■

If you'd like to comment on this subject please write to the Editor at ***Svetlana.josifovska@stjohnpatrick.com***

The End of Electric Charge and ELECTRIC CURRENT as We Know Them

Ivor Catt, an engineer and a scientist, presents a two-part article on the matters of electrical charge and current. This is the first part, with the second part to follow in the next issue of *Electronics World*

FOR 43 YEARS it has not been noticed, even by the author, that oscilloscope pictures (reproduced here) in a refereed journal undermine the concepts of electric charge and electric current, and with them a large part of 20th century scientific theory. We see two electric currents travelling in opposite directions down a single conductor. Conventional electric current is not fit for purpose.

Under Faraday's Law $(V = -\frac{d\phi}{dt})$, which forbids superposition and yet whose mathematics permits it, we end up with two electric currents travelling in opposite directions down the same conductor.

In **Figure 1**, I inject a very narrow voltage spike between the left hand surface conductor and the ground plane. The bottom trace in the left-hand **Figure 3** shows the introduced voltage spike, and the bottom trace in the right-hand Figure 3 shows the smaller spike immediately resulting in the right hand conductor. The later second and first traces show how the signal develops further along the pair of conductors. It separates out into, first, an Odd Mode signal with equal and opposite voltage spikes on the pair of lines, followed by a slower Even Mode signal of equal positive spikes.

In **Figure 2**, the case of buried conductors, the two modes travel at the same velocity and do not separate out, as shown in **Figures 5** and **6**. Now let us look at the case of surface conductors when the front end of the right hand passive conductor is shorted to ground so that there can be no voltage there.

In **Figures 7** and **8** we see that in the earliest, bottom traces the initial zero voltage in the right hand conductor must have been two equal and opposite voltages superposed. At the same time, there must have been equal and opposite charges on the surface of the right hand conductor, and equal and opposite electric currents flowing in and out of this conductor. As we see in **Figure 9** in the field patterns, in the Even Mode the right hand conductor is positive and so electric current flows into the paper, generating the field pattern shown. Meanwhile, in the Odd Mode, the right hand conductor is negative so electric current flows out of the paper.

Looking back, this must have been happening in all traces in Figures 5 and 6 and in the bottom traces in Figure 3.

First, assuming a TEM Wave, I mathematically prove that only one voltage/current ratio and one velocity can travel down between a conductor and ground plane.

Properties of a Transmission Line

I've called this section 'Properties of a transmission line' or 'Proof that only one type of wave-front pattern can be propagated down a two-wire system'.

In order to discover how we characterize a transmission line we shall consider an observer watching a step passing him along a two-wire line (see **Figure 10**).

The observer knows: (a) Faraday's Law of Induction and (b) that electric charge is conserved.

Use Faraday's law $(V = -\frac{d\phi}{dt})$ around the loop AA'B'B. Define l as the inductance per unit length of the wire pair, then:

$$l = \frac{\phi}{i} \quad (1)$$

In a time δt, the step will advance a distance δs, such that:

$$\frac{\delta s}{\delta t} = C \quad (2)$$

and the change of flux will be (from **Equation 1**):

$$\delta\phi = l\,\delta s\, i \quad (3)$$

Substitution into (a) Faraday's Law gives the input voltage V across AB needed to equal and overcome the back e.m.f. $v_{back} = \frac{\delta\phi}{\delta t}$.

From **Equations 2** and **3**:

$$v = v_{back} = l\, i \frac{ds}{dt} = l\, iC \quad (4)$$

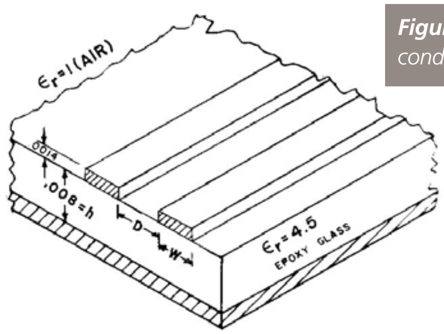

Figure 1: *Surface conductor (Microstrip)*

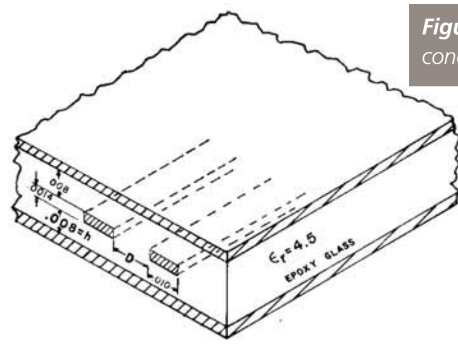

Figure 2: *Buried conductor (Stripline)*

Now we consider the conservation of charge. In a capacitor in general, $q = cv$. In our case, the charge $i\delta t$ entering the line in time δt equals the charge trapped in charging up the next segment δs of the line, $c\delta s\, v$ where c is the capacitance per unit length between the pair of wires and $c\delta s$ is the capacitance of our section.

$$i\delta t = vc\delta s, \text{ which means that } i = vcC \quad (5)$$

Combining **Equations 4** and **5**:

$$vi = l\, iC\, vcC$$

$$C = \pm \frac{1}{\sqrt{lc}} \quad \left[= \pm \frac{1}{\sqrt{\mu\varepsilon}} \right] \quad (6)$$

$$\text{and } \frac{v}{i} = Z_0 = \sqrt{\frac{l}{c}} \quad (7)$$

Thus we see that, knowing only Faraday's Law and that charge is conserved, the observer in Figure 10 concludes that any step passing him must have a single velocity *C* and a single voltage-current relationship given by an 'Ohm's Law' type relation:

$$\frac{v}{i} = Z_0 \quad (8)$$

where Z_0 is a property of (1) the geometry of a cross-section of the wires and (2) of μ and ε characteristics of the medium in which the wires are embedded.

Crosstalk in Digital Systems

This sections is 'Crosstalk in digital systems' or proof that only two types of wave-front pattern can be propagated down a system of two parallel wires and a ground plane.

In **Figure 11** the method of images is used; it is assumed that $i_b = -i_a$, $i_q = -i_p$.

The following terms are defined for steady state conditions:

l = Magnetic flux per unit length between AA' and BB' when unit current flows down AA' and back on BB'.

m = Magnetic flux per unit length between AA' and BB' when unit current flows down PP' and back on QQ'.

c = Charge per unit length on AA' and BB' which produces unit voltage drop between AA' and BB'=l/(coefficient of capacitance).

d = Charge per unit length on AA' and BB' which produces unit voltage drop between PP' and QQ'=1/(coefficient of induction).

This could well be called "Mutual Capacitance".

In order to discover how we characterize the four wire system we shall consider an observer watching a step passing him (**Figure 12**).

The observer knows: (a) Faraday's Law of Induction and (b) that electric charge is conserved.

Now assume that the wave front passing him involves current steps i_a and i_p travelling down the lines with a velocity *C*.

From $v = \frac{d\phi}{dt}$ between AA' and BB', we get (as in Equation 4):

$$v_{ab} = l\, i_a C + m\, i_p C \quad (9)$$

Similarly $v = \frac{d\phi}{dt}$ between PP' and QQ', so:

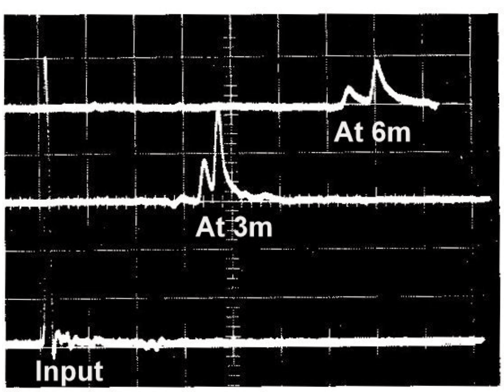

Figure 3a: *Signal on active left hand line*

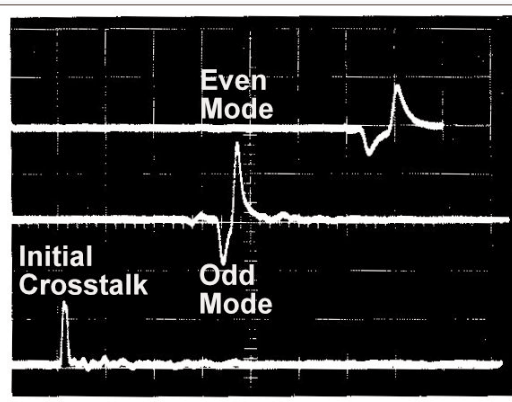

Figure 3b: *Signal on passive right hand line*

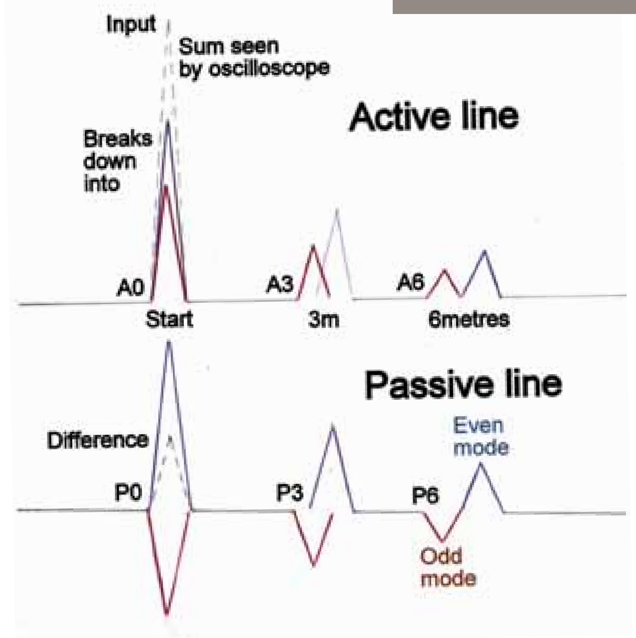

Figure 4: *Drawings of Figure 3*

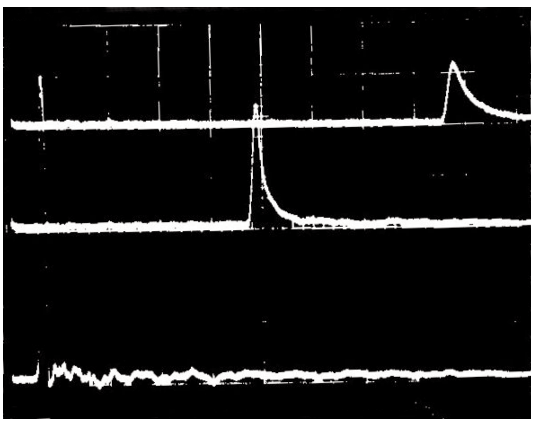

Figure 5: *Signal on active left buried line*

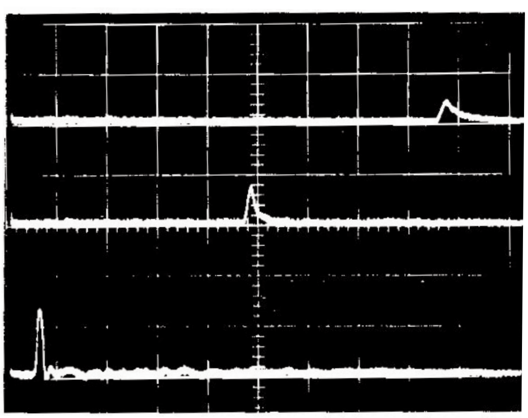

Figure 6: *Signal on passive right buried line*

$$v_{pq} = l\, i_p C + m\, i_a C \quad (10)$$

Also, from v=q/c (as in Equation 5):

$$v_{ab} = \frac{i_a}{cC} + \frac{i_p}{dC} \quad (11)$$

$$v_{pq} = \frac{i_p}{cC} + \frac{i_a}{dC} \quad (12)$$

First find C. Eliminate voltages from **Equations 9** through to **12**. From Equations 9 and 11 we get:

$$l\, i_a C + m\, i_p C = \frac{i_a}{cC} + \frac{i_p}{dC}$$

$$l\, i_a C^2 + m\, i_p C^2 = \frac{i_a}{c} + \frac{i_p}{d}$$

Therefore:

$$\frac{i_a}{i_p} = -\frac{m C^2 - \frac{1}{d}}{l C^2 - \frac{1}{c}} \quad (13)$$

Similarly, from **Equations 10** and **12** we get:

$$\frac{i_a}{i_p} = -\frac{l C^2 - \frac{1}{c}}{m C^2 - \frac{1}{d}} \quad (14)$$

Eliminate i_a and i_p from **Equations 13** and **14** to get:

$$C = \pm\sqrt{\frac{\frac{1}{c} + \frac{1}{d}}{l + m}} \text{ or } \pm\sqrt{\frac{\frac{1}{c} - \frac{1}{d}}{l - m}}$$

So in the forward direction there are two possible velocities of propagation:

$$C_e = +\sqrt{\frac{\frac{1}{c} + \frac{1}{d}}{l + m}}$$

or:

$$C_0 = +\sqrt{\frac{\frac{1}{c} - \frac{1}{d}}{l - m}}$$

Returning to Equation 13 and using the results for C, we find that the following two wave fronts are possible: The EM, or Even Mode, wave (**Figure 13**) is like a TEM step travelling down between two wires made up of A shorted to P and B shorted to Q. It has the higher Z_0 and (in the case of surface, or stripline, conductors) the lower velocity (because more of its field is in the slower medium of epoxy glass).

$$C_e = +\sqrt{\frac{\frac{1}{c}+\frac{1}{d}}{l+m}}$$

$$Z_{0e} = \sqrt{(l+m)\left(\frac{1}{c}+\frac{1}{d}\right)}$$

$$i_a = i_p$$

$$v_{ab} = v_{pq} \qquad (15)$$

OM Wave

The OM, or Odd Mode, wave (**Figure 14**) is like a TEM step travelling down between two wires made up of A shorted to Q and P shorted to B.

$$C_0 = +\sqrt{\frac{\frac{1}{c}-\frac{1}{d}}{l-m}}$$

$$Z_{00} = \sqrt{(l-m)\left(\frac{1}{c}-\frac{1}{d}\right)}$$

$$i_a = -\,i_p$$

$$v_{ab} = -\,v_{pq} \qquad (16)$$

Our initial assumption in our mathematics was that a stable waveform passed the observer; that is, a TEM wave which was in equilibrium or, as Einstein put it, "at rest". (See *"Einstein's Error"* in the next issue of *Electronics World*).

Following that assumption, we used Faraday's Law and concluded from our calculations that no other waveform may pass the observer other than the Even Mode and the Odd Mode. However, superposed combinations of EM and OM are permissible, as are seen in Figures 5 and 6. They are permissible in the real world, but not permissible according to Faraday's Law, which is therefore not about the real world as photographed here.

This mathematics was "confirmed" by the upper two traces in Figures 3, 7 and 8. However, for 43 years I failed to notice that the bottom traces in these figures, and all the traces in Figures 5 and 6 give an illegal asymmetrical, third mode, which is a combination of an Even Mode and an Odd Mode. On their own, Even Mode and Odd Mode are symmetrical with respect to the four conductors.

At Odds

Clearly, physical reality was disproving a conclusion derived mathematically from Faraday's Law, that only the Even Mode and the Odd Mode were permissible. The mathematics is indifferent as to whether superposition is permissible. It does not cover all the features of the physics.

Faraday's Law (but not its maths) outlaws the superposition of two permissible modes, which become a third, illegal mode. One reason why it is illegal is that the electric currents in the right-hand conductor are in opposite directions for the two modes, and classical theory says there cannot be two electric currents in opposite directions along a single conductor. However, two electromagnetic waves (or light rays) can be in the same point in space, for instance when we shine a torch at another lighted torch pointing in the opposite direction, or when we send two

Figure 7: *Signal on active left line with right line shorted to ground*

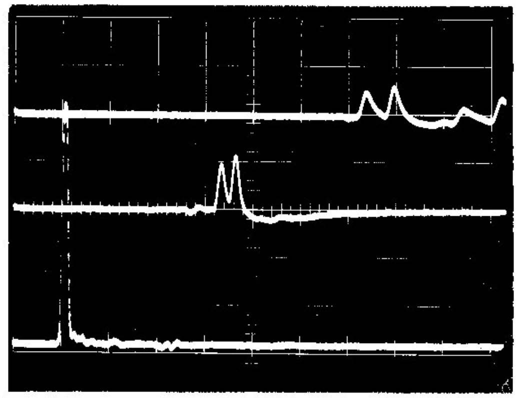

Figure 8: *Signal on passive right line with its front end shorted to ground*

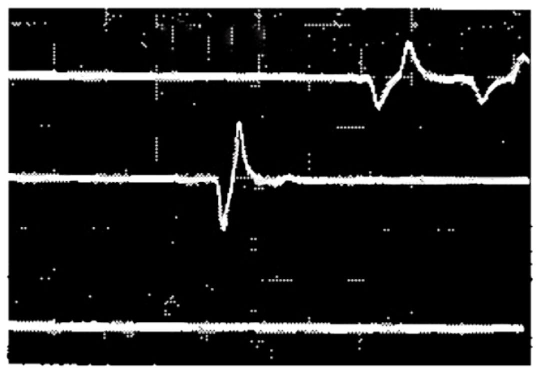

Figure 9: *Field patterns for Even Mode and Odd Mode for surface lines. It is simpler to think of four conductors rather than two conductors and a ground plane*

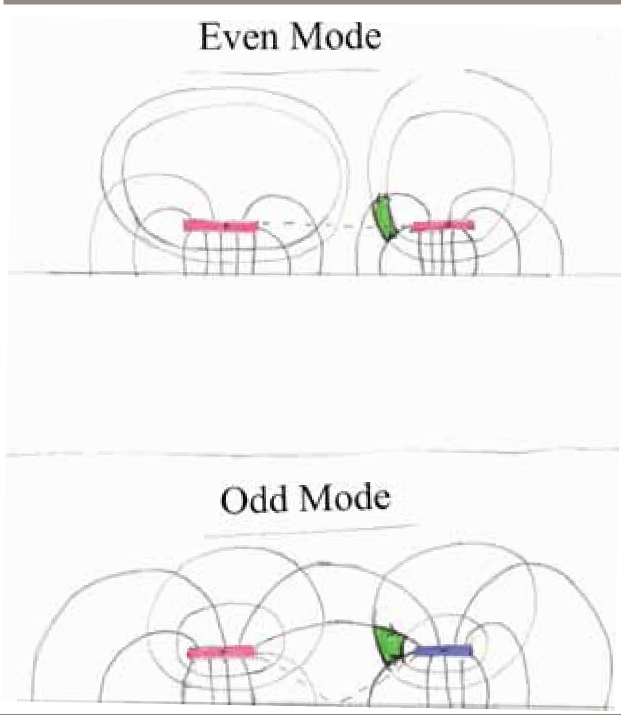

Figure 10: An observer watching a voltage step passing him along a two sire system

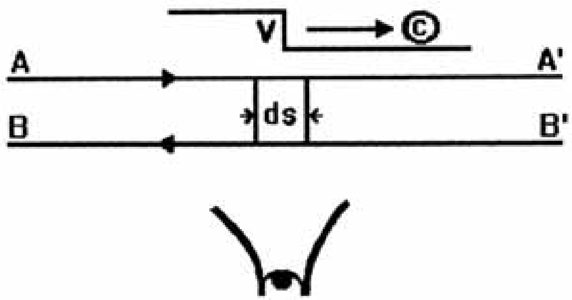

Figure 12: An observer watching a voltage step passing him along a four wire system

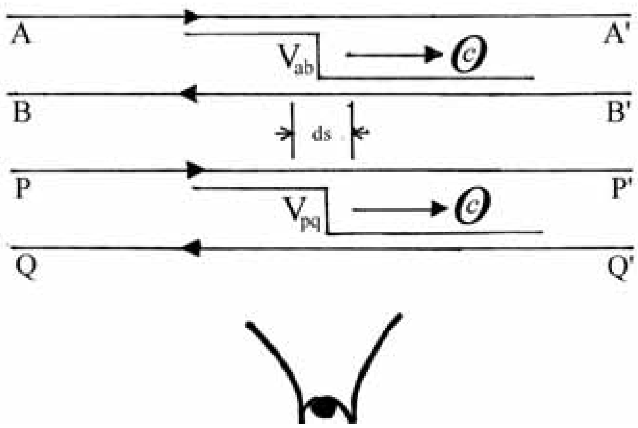

Figure 14: Illustration of the Odd Mode

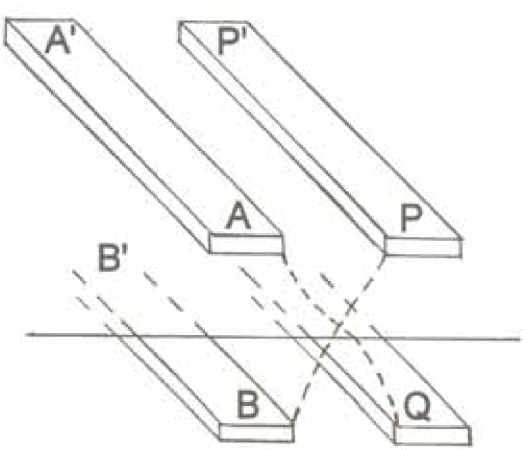

Figure 11: A pair of parallel surface lines and their images

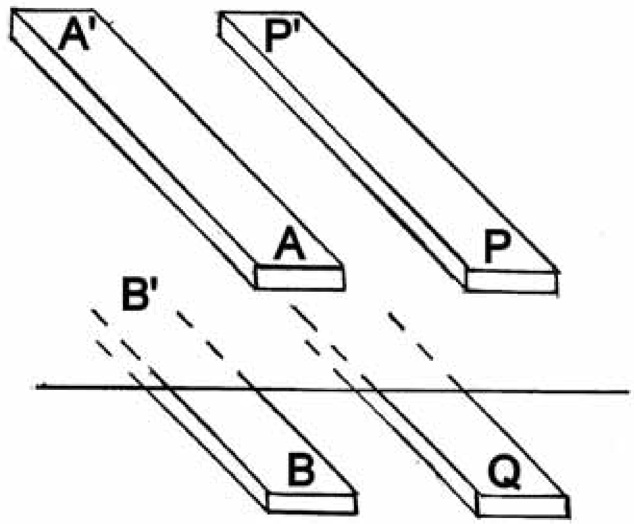

Figure 13: Illustration of the Even Mode

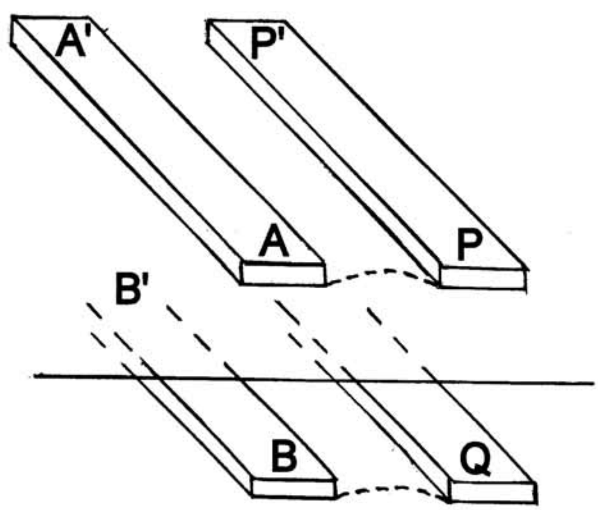

pulses from left and right through each other down a coaxial cable.

The figures show that the Even and Odd Mode TEM Waves can coexist, but not their associated electric charges and currents. To resolve the problem, we study the mathematics of it next month.

The second-part of Ivor Catt's article continues in the next issue of Electronics World magazine.

Transmission Line TRANSIENTS

Here **Ian Darney** answers the question of '*When a voltage step travels down a transmission line at the speed of light guided by two conductors, where does the negative charge come from on the bottom conductor to terminate the electric field between the conductors?*'

EVERY NOW AND again a particularly intriguing question is raised in the pages of *Electronics World* (EW):

'*When a voltage step travels down a transmission line at the speed of light guided by two conductors, where does the negative charge come from on the bottom conductor to terminate the electric field between the conductors?*'. (The Catt Question, Letters, EW May 2009).

It would seem logical to look for the answer in books on electromagnetic theory. After all, it is in these books that the concept of a travelling wave is introduced, and where a circuit model is described which replicates the mechanisms involved in transmitting a signal along a pair of conductors.

What follows is a description of an experiment carried out to compare the performance of an actual transmission line with the response predicted by theory. It just happened that the subsequent analysis provided an answer to the above question.

The experiment utilised low-cost equipment that should be familiar to the vast majority of readers of EW, and can be repeated by anyone willing to do so. It can be guaranteed that anyone who accepts this challenge will acquire a much deeper understanding of interference coupling mechanisms and will be able to improve the EMC of any equipment he or she is likely to design in future.

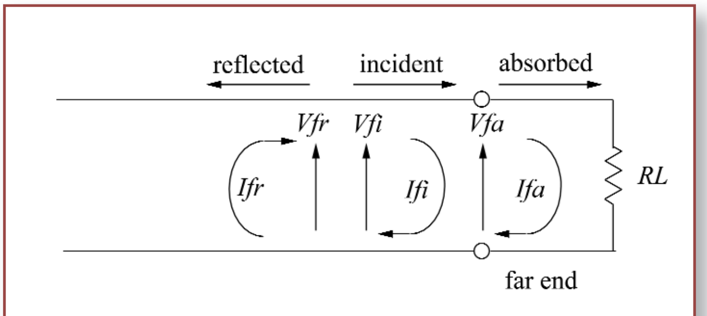

Figure 1: *Currents and voltages at the far end of the line*

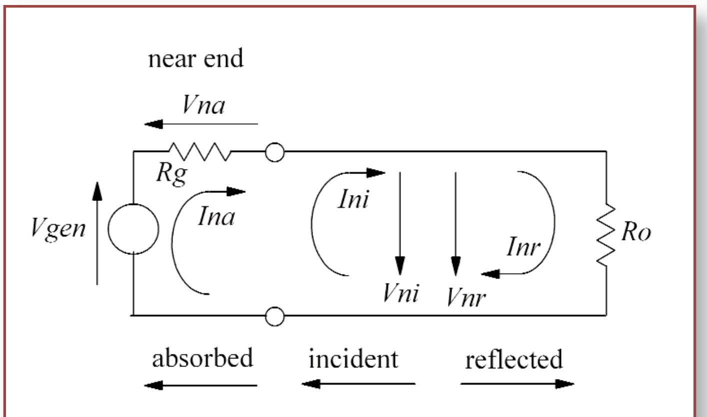

Figure 2: *Currents and voltages at the near end of the line*

Interactions

Figure 1 illustrates the interactions which take place when a signal reaches the receiving end of a transmission line. The concept of partial parameters is introduced to distinguish between incident and reflected currents and voltages. The convention adopted here is that positive current flows clockwise.

Since the currents and voltages at the far end are usually different from those at the transmitting end, it is necessary to assign them separate identities. Hence, Ifa is 'the amplitude of the current which is absorbed by the load resistor RL at the far end of the line'. The relationships are:

$$Ifr = \frac{(Ro - RL) \cdot Ifi}{Ro + RL} \qquad (1)$$

and

$$Ifa = Ifi + Ifr \qquad (2)$$

where Ro is the characteristic impedance of the line. The figure also illustrates the fact that loop currents are involved; current flowing along one conductor is precisely matched by current flowing in the opposite direction in the other conductor.

Figure 2 illustrates the model representing the sending end of the line.

Here, the relationships are:

$$Inr = \frac{(Ro - Rg) \cdot Ini + Vgen}{Ro + Rg} \qquad (3)$$

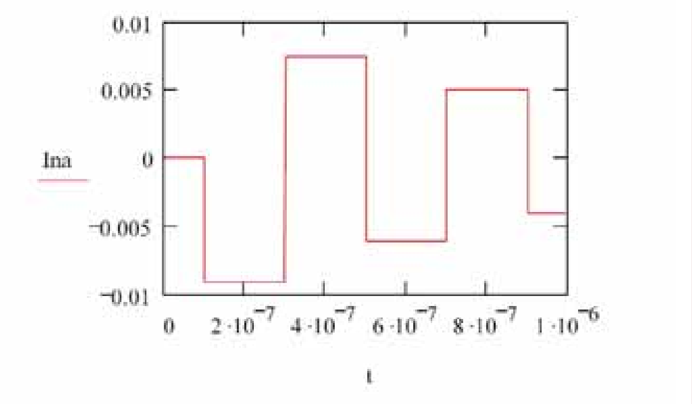

Figure 3: *Predicted current waveform due to step voltage input*

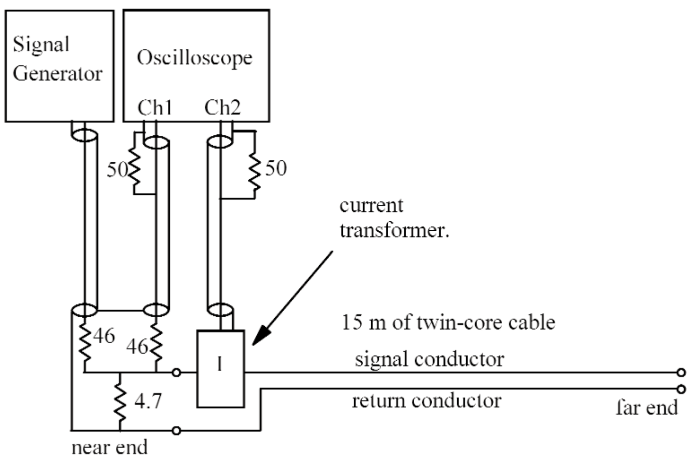

Figure 4: *Set-up for radiated transient test*

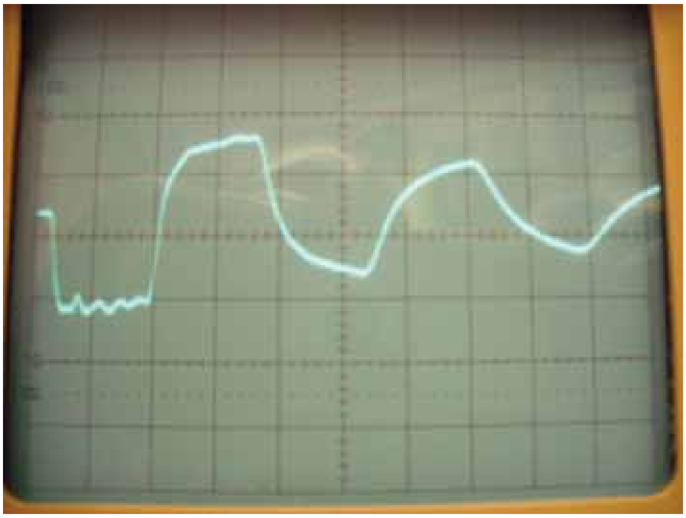

Figure 5: *Current waveform, as monitored on channel 2 of the oscilloscope*

and

$$Ina = Ini + Inr \tag{4}$$

The partial current Inr propagates at a velocity v along the line and arrives at the far end after time T, where:

$$T = \frac{l}{v} \tag{5}$$

and l is the length of the line. Hence, after an elapsed time T:

$$Ifi \leftarrow Inr \tag{6}$$

and

$$Ini \leftarrow Ifr \tag{7}$$

Time-step analysis can be used to simulate the action of the line. Given a characteristic impedance of 100 ohm, a time constant of 100ns, a source impedance of 10 ohm and open-circuit terminations at the far end, the current Ina, when the source voltage steps from zero to -1V, would be as illustrated by **Figure 3**.

Setup

The ultimate check on the validity of any circuit model is to compare its response to that of an actual transmission line. So this was done. **Figure 4** illustrates the setup.

A length of mains cable was selected for the test, since such cable is reasonably representative of many interconnections used in electronic equipment. A relatively long cable (15m) was used, to ensure the monitored waveform was comparable with that of Figure 3. The resistor network at the near end was designed to provide very low source impedance, and the far end of the line was left open-circuit.

Such a configuration ensures that multiple reflections occur. It is the reflected signal which provides information as to what happened to the wavefront in its traverse from near end to far end. If there are no reflections, then that information is lost.

The signal generator was set to give a square wave, and the frequency was set low enough to allow conditions to settle between the leading and trailing edges.

Channel 1 of the oscilloscope was used to monitor the waveform of the input voltage at the near-end terminals. The amplitude of this waveform was used to set the magnitude of Vgen in the model of Figure 2. Channel 2 was used to monitor the waveform of the current delivered to the line; that is, the current Ina of the circuit model.

Figure 5 is a photograph of the waveform monitored by channel 2. Scaling was 100nS/div and 10mV/div. This gives the time delay between first and second edges as 166ns, indicating that the time taken for the first edge to propagate to the far end was 83ns. During this period, there is a ripple on the waveform due to discontinuities along the line.

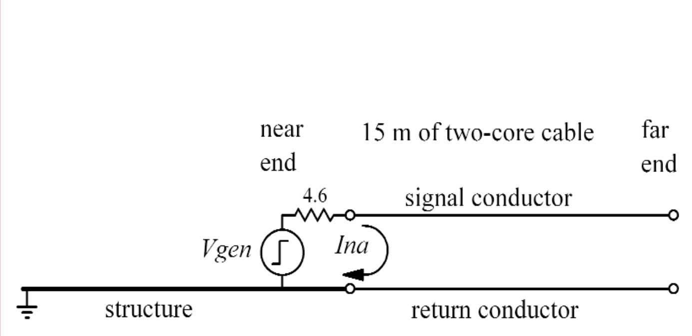

Figure 6: Simplified model of the setup

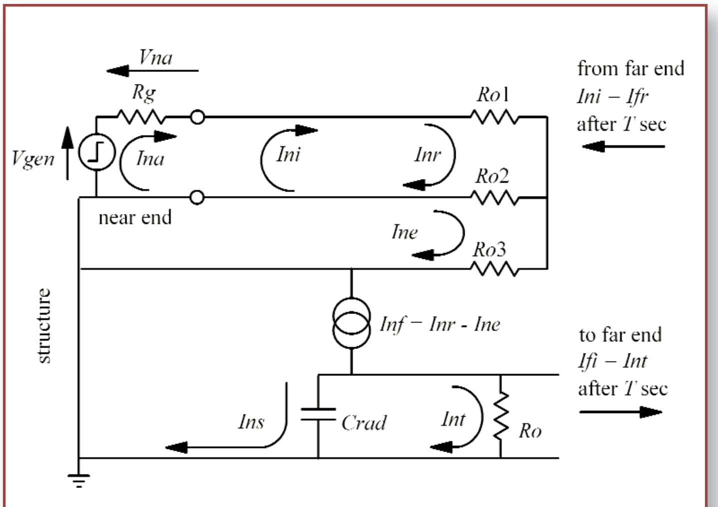

Figure 7: General circuit model for transient emissions

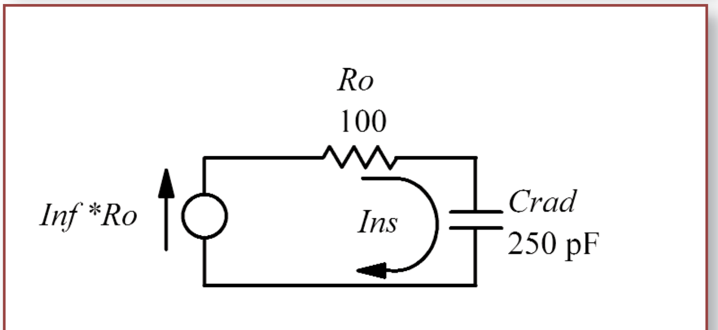

Figure 8: Calculating the value of the stored current

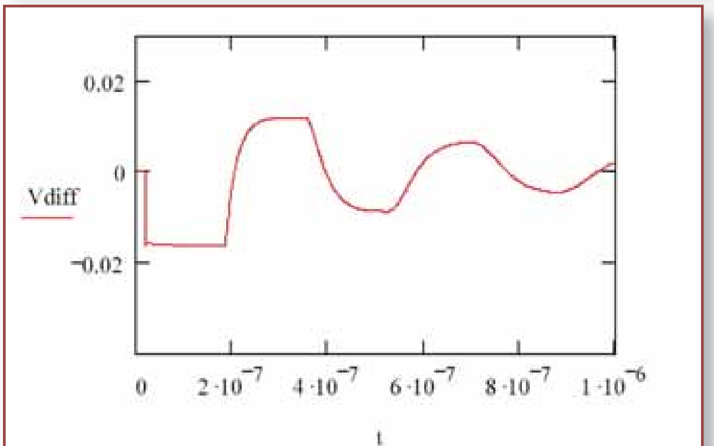

Figure 9: Response of circuit model of Figure 8

These discontinuities created reflections which arrived back at the near end long before the initial transient returned from the open-circuit termination.

When the current transient reaches the far end, it appears as incident current Ifi. Since this termination is open-circuit, this current is reversed in sign and reflected straight back towards the near end. When it reaches the near end, its amplitude is almost doubled. This means that the waveform of the trailing edge is a magnified, inverted, reproduction of the waveform which arrived at the far end T seconds previously.

Comparisons

Comparing the shape of the first trailing edge of Figure 5 with that of Figure 3 reveals that, instead of the expected sharp step from a negative value to a positive value, the transition follows an exponential rise. This means that a significant portion of the current leaving the near end does not arrive at the far end.

The exponential waveform indicates that the 'lost' current has been absorbed by a capacitor. Since the same mechanism applies to every change in amplitude of the current, the waveform gradually changes from a square wave to a sine wave.

If the losses had been due to current flow in the dielectric material of the cable insulation, then the effect could have been simulated by a resistance in parallel with the characteristic impedance Ro. If such a modification had been applied to the circuit model, then the amplitude of the current Ina would have decreased more rapidly, but the edges of the waveform would still have been quite sharp. Hence, the waveform of Figure 5 cannot be explained by assuming it is due to lossy insulation.

Only one explanation is possible: current is flowing from the transmission line into the environment. The line is acting as an aerial. This should be no surprise to anyone who has experienced the effect of transient interference.

Figure 6 is a simplified model of the setup. The structure, generator, 4.6 ohm resistor and signal conductor can be viewed as a dipole aerial. When a step voltage is applied, the initial current flow is along the signal conductor. This sets up an electromagnetic field which spreads out, rather like the bow wave of a ship. After about a pico-second, it arrives at the return conductor and creates an opposing charge on the surface. The voltage due to this charge creates a current which flows back towards the near end. Current in the return conductor creates its own electromagnetic field which couples with the signal conductor.

Not all of the field emanating from the signal conductor couples with the return conductor. Hence, the amplitude of the current in the return conductor is less. Moreover, not all of the field emanating from the return conductor couples with the signal conductor. The return conductor is also a source of radiation. This means that, as well as the differential-mode components illustrated in Figure 2, there is an additional aerial-mode current flowing in the cable.

This aerial mode current can be simulated by replacing the characteristic impedance Ro of Figure 2 with the potentiometer network of **Figure 7**. In this model, Ro1 represents the characteristic impedance of the signal conductor, Ro2 represents the return conductor and Ro3 represents the effect of the environment. The relationship is:

$$Ro = Ro1 + \frac{Ro2 \cdot Ro3}{Ro2 + Ro3} \qquad (8)$$

The aerial-mode current emitted into the environment is:

$$Ine = \frac{Ro2}{Ro2 + Ro3} \cdot (Ini + Inr) \qquad (9)$$

That is, current is emitted into the environment by the incident current as well as by the reflected current. Since this current has departed from the cable, the remaining current flowing from the near end to the far end must be:

$$Inf = Inr - Ine \qquad (10)$$

Not all of this current actually reaches the far end. The fact that aerial-mode current is flowing means that an aerial-mode charge builds up along the cable. Current used to store this charge is simulated by Ins in Figure 7. Since a current source in parallel with a resistor can be replaced by a voltage source in series with that resistor, the magnitude of Ins can be determined from the model of **Figure 8**.

So:

$$Ins = Inf - \frac{Qns}{Ro \cdot Crad} \qquad (11)$$

The value of the stored charge is determined by adding its value a short time dt in the past to the amount of charge added during that time. It can be calculated using the computer statement:

$$Qns \leftarrow Qns + Ins \cdot dt \qquad (12)$$

This means that the current actually transmitted to the far end must be:

$$Int = Inf - Ins \qquad (13)$$

So, after an elapsed time T:

$$Ifi \leftarrow Int \qquad (14)$$

Defined by Equations

Both conductors at the far end are isolated from ground. Aerial-mode current incident at the far end must be zero, since all of it has departed into the environment. There can be no reflected aerial-mode current at this pair of terminals. So the response at the far end is the same as that defined by **Equations 1** and **2**.

Collecting all these equations together in a computer program which invokes time-step analysis leads to a waveform defining the response of the model of Figure 7. This is illustrated by **Figure 9**.

Comparing Figure 5 with Figure 9 demonstrates that the response of the new circuit model provides a reasonably accurate simulation of the performance of the configuration-under-review. This being so, it effectively validates the reasoning used in the development of the model.

The value of the emitted current is defined by the parameter Ine, and is related to the current delivered to the cable by **Equation 9**. Since the ratio of resistance values is a pure number, the radiated current Ine must be a fraction of the differential-mode current Ina. That is, the waveform of the radiated emission is identical to that of the differential-mode signal.

The value of the stored current is defined by the amplitude of Ins and calculated using **Equation 11**. Since the energy is stored as a voltage across the radiation capacitor Crad, it does not radiate out into the environment immediately. However, it does not remain in storage for long. The charge held by Crad re-appears as aerial-mode current delivered by the line to the circuitry at the near end. This incident current is immediately reflected back into the environment.

Answering the Questions

So, to answer the question posed at the start of this article; the negative charge on the bottom conductor comes from electromagnetic radiation emanating from the top conductor.

The source of the energy is the voltage generator at the near end of the cable. The structure and signal conductors behave in essentially the same way as two poles of a dipole transmitting aerial; current drawn from one conductor flows directly into the other.

It is not at all difficult to repeat the experiment described above. Function generators and oscilloscopes are low-cost items of general-purpose test equipment. If a current transformer is not immediately available, one can be constructed by winding ten turns of enamelled copper wire onto a ferrite toroid and connecting a 51 ohm resistor between the terminations.

Detailed descriptions of the construction of the current transformer and its calibration can be found in section 7.2 of the book "*Circuit Modelling for EMC*". This is freely available at **www.designemc.info**. The test itself is described in section 7.6 and the Mathcad worksheet used to simulate the response of the model is described in section 6.6. There is also a webpage which allows the program to be downloaded. ■

Smart Experimental Management System for Electrical and Electronic ENGINEERING LABORATORIES

N. Suha Bayindir of the Eastern Mediterranean University, **Ilker Degirmencioglu** of Enot Electronic Ltd and **H. Ozgur Bayindir** of the Middle East Technical University present a Smart Experimental Management System (SEMS) as a compact intelligent laboratory control system

THE CONVENTIONAL experimental systems available at present at universities and technical colleges are generally inflexible, instruction-based and closed ended systems, which enable neither the instructor nor the student to modify the experimental procedures, or permit the development of new procedures.

The Smart Experimental Management System (SEMS) has many novel and original features which are superior to those of current experimental sets and provides solutions to overcome the drawbacks of these sets. Moreover, with its software configured flexible nature, it can be continuously upgraded and adapted to new technologies and methods, according to the demands and suggestions of the instructors.

SEMS is designed to enable students of engineering and polytechnical schools to learn the principles of systems in areas involving electrical, electronic, microprocessor, control, electromagnetic and mechanical components, easily, with interest and fun. Due to the digital and flexible operating system of the SEMS, all experimental measurements can be transferred to the computer environment; experimental scenarios can be arranged according to the desires of the instructors; and experiments which will develop the creative abilities of the students can be produced. SEMS has a flexible nature which can be adopted to state-of-the-art technology, with very simple hardware and software modifications.

Although the system was primarily intended to be used in Electrical, Electronic and Computer Engineering Laboratories, owing to its data acquisition and software capabilities, it can easily be adapted to other disciplines such as the Basic Sciences and Biomedical Applications.

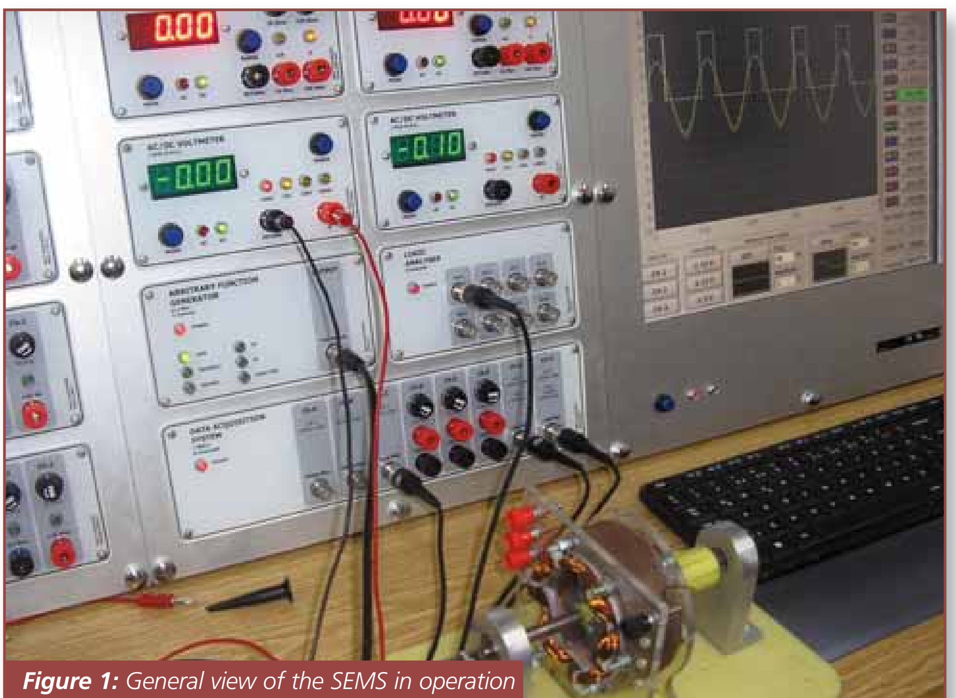

Figure 1: *General view of the SEMS in operation*

Characteristic Features of SEMS

SEMS, illustrated in **Figure 1**, is an Intelligent Experimental Data Management System, equipped with a built in microcomputer-based Data Acquisition and Control System which enables all experimental procedures to be performed in a digital environment and where all measured data can be monitored on an LCD display and stored in memory for further processing.

Characteristic curves and tables can be easily produced, analyzed and reported in the digital environment of the SEMS. This allows the student more time and a friendly user interface to discover and apply new experimental procedures and to correlate various measured quantities such as voltage (V), current (I), torque (T) and speed (n). As a result a student will have the chance of developing his/her creative abilities while comprehensively understanding all features of the system under test.

Due to its digital and flexible structure, experiments can be custom designed, merged and interlinked according to the requirements of the lecturer. Open ended experiments can be assigned to students and experiments can be easily upgraded to apply to newly emerging technologies.

Animations are provided to illustrate complicated principles of operation of magnetic and electromechanical devices which will enable students to understand all theoretical and operational aspects of experiments before they attend the laboratory session.

Hardware and Software Components

SEMS consists of a DAQ card, AC/DC power supplies, measuring instruments and an intelligent management software that provide many functions to perform an interactive and instructive experiment. The user friendly interface of the SEMS enables the students to use the Experimental Management Software for viewing, analyzing and storing the measured data obtained during the experimental work. Moreover, the SEMS Experimental Software guides the student with user defined experimental scenarios and illustrates the important aspects of the experiment with animations.

Unlike the conventional oscilloscopes, SEMS enables the observation of 8 variables which may or may not have common grounds, simultaneously on 4 different graphical charts whose axis can easily be defined by the user according to the type of the measured data. Transient as well as steady state measurements can be stored and displayed on the same graph. Characteristic curves are automatically generated by the software without needing any manual operation.

Figure 2: *General layout and the actual view of the DAQ card*

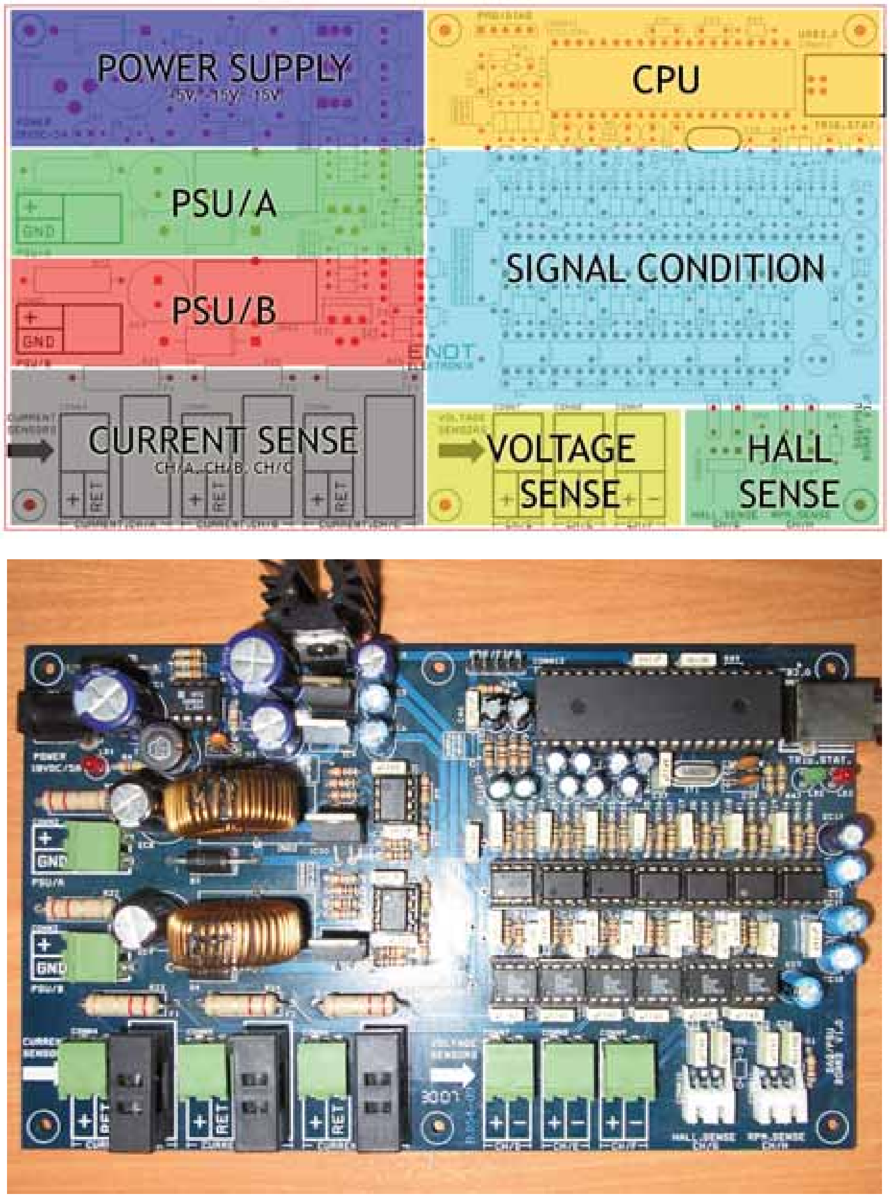

All power supplies, DAQ input terminals, measuring instruments and the touch panel LCD display are mounted on the front panel of the SEMS which provides a tidy environment where very little cabling is required during the experiments and maintenance of equipment is minimized; this is the opposite of experiments with individual equipment which may easily be broken, stolen or suffer from frequent battery failures.

There are two fixed DC power supplies and a three-phase, variable AC power supply with digital voltage and current displays, overcurrent limit and short-circuit protections. The power supplies of SEMS are isolated with a central isolation transformer and, together with earth leakage circuit breakers, provide a very safe experimental environment for the students. All equipment is supplied with over-current and short circuit protection which protects the circuits without blowing the fuses and causes least interruption time.

SEMS incorporates a software Arbitrary Function generator which can produce any user-defined signal appropriate to the experimental procedure. The waveform of any mathematical function that is typed on the user interface textbox is automatically generated by the SEMS. This feature eliminates the limitations of conventional signal generators which can generally produce only sinusoidal, triangular and

Figure 3: Isolation amplifier circuit

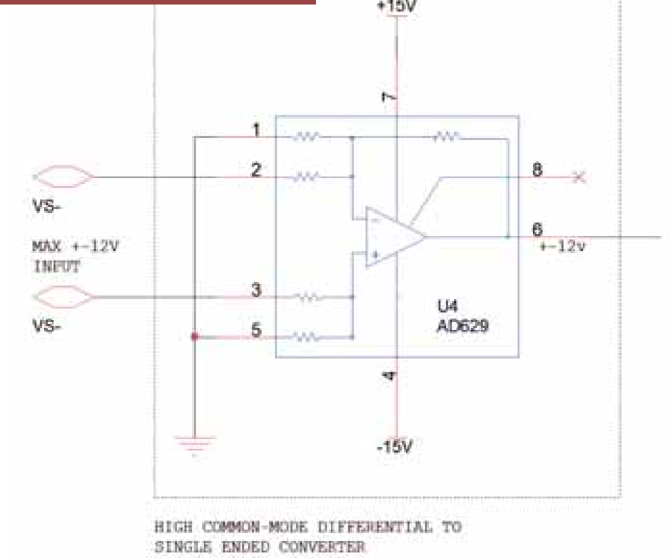

square waveforms and allows all sorts of signals to be generated which are very useful in experimental or research work concerning signal processing applications.

The measured results can be monitored either using the smart analysis, display and reporting features of the SEMS software, or using the 8-channel, storage type, colour oscilloscope and the logic analyzer created by the SEMS software on the touch panel LCD display.

DAQ Card Design Features

The Data Acquisition Card of the SEMS is designed to receive the analogue measured data from the experimental sets, condition the measured data according to the analogue input requirements of the microcontroller which is then used to convert the measured data into digital form. This data is then transferred to the host computer via the USB port, where the measured data is processed to provide the required characteristic curves which can be monitored on the LCD display or printed if required. The microcontroller is also used to control the operation of the input channels and to program the digital power supply units.

The DAQ card has 3 isolated analogue voltage and 3 isolated analogue current channels, 1 Hall-effect input channel for flux measurements, 1 channel for speed or frequency measurements and 8 digital I/O channels. The Instrumentation and Control software of the SEMS provides an 8-channel colour software storage oscilloscope, an 8-channel Logic Analyzer, a programmable Switched Mode Power Supply (SMPS) and a variable AC supply which can be configured and monitored on a touch panel LCD display.

Figure 2 shows the general layout of the DAQ Card which consists of switched mode power supplies to provide ±15V and ±5V fixed DC supply and a linear source-sink type, three phase power supply to provide 0-30V AC variable voltage, a microcontroller, signal conditioning circuits and the voltage, current and Hall-effect sensing input channels to convert analogue experimental data into digital form for further processing.

The digital power supply units are of the DC/DC SMPS type and provide higher efficiency and better regulation than those using linear regulators. The maximum current rating of the power supplies is 3A, which is sufficient for most of the electrical, electronic and computer engineering applications. Software controlled soft-start and current limiting techniques, are used to limit the starting current of electrical motors to a value below the rated current of 3A.

Resistors of 0.1 Ohm are connected in series with the current input channels to enable the measurement and monitoring of the measured currents. It is very likely that inexperienced students may overload the

Figure 4: Current input channel signal conditioning

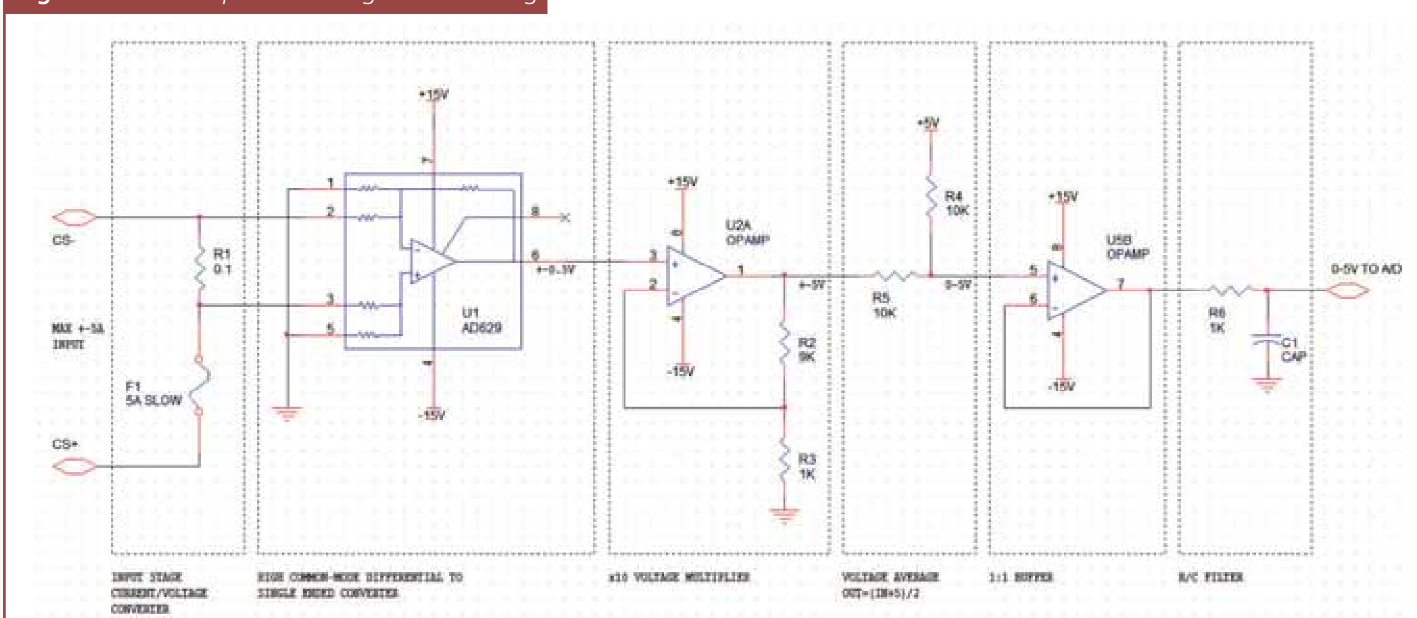

input channels by making simple connection mistakes, hence the current channels should be well protected. These channels are protected by software-controlled current limiting and short circuit protection methods as well as a 5A fuse, thereby making the input channels virtually student-proof.

The voltage input channels on the bottom right of the DAQ card are protected against transient voltages up to ±500V and to ±270V in the steady-state condition. This protection also provides isolation (up to 270V) between the voltage channels and enables the simultaneous measurement of voltages with respect to different reference points at various points of an experimental circuit.

This is a novel feature of the SEMS making it superior to conventional measuring instruments such as oscilloscopes, spectrum analyzers and logic analyzers where measurements can be taken only with respect to common ground.

The novel voltage protection/isolation method can be described with reference to **Figure 3** as follows: The voltages of the two inputs, across which the differential voltage will be measured, are reduced by a factor of 20 with respect to the potential of the case, by using very accurate (laser trimmed) voltage divider resistors. These voltages are then converted into single-ended signals relative to the potential of the case, by using a high precision differential amplifier type AD629. Even though there is no actual electrical isolation in this scheme, all differential voltages can be measured safely, as long as the difference between channel voltages does not exceed 270V (which is valid in the majority of experiments).

Current Channels

There are three independent Current Input Channels on the DAQ Card, each of which is capable of measuring ±5A with an isolation level between channels of up to 100V. The current is sensed as a voltage drop across a 0.1 Ohm, 5W series resistor with an accuracy of 0.1%. The sense range is -5/+5 amps, where the maximum power dissipation in the resistors is 2.5W, and a slow acting fuse in series with the resistor is used for protection purposes.

To provide isolation up to 100V between current input channels, the voltage difference between channels is routed to a High Common-Mode Voltage Difference Amplifier type AD629, which is a direct replacement for INA117 series amplifiers

Figure 5: *Graphical display of test results for a 75W DC motor*

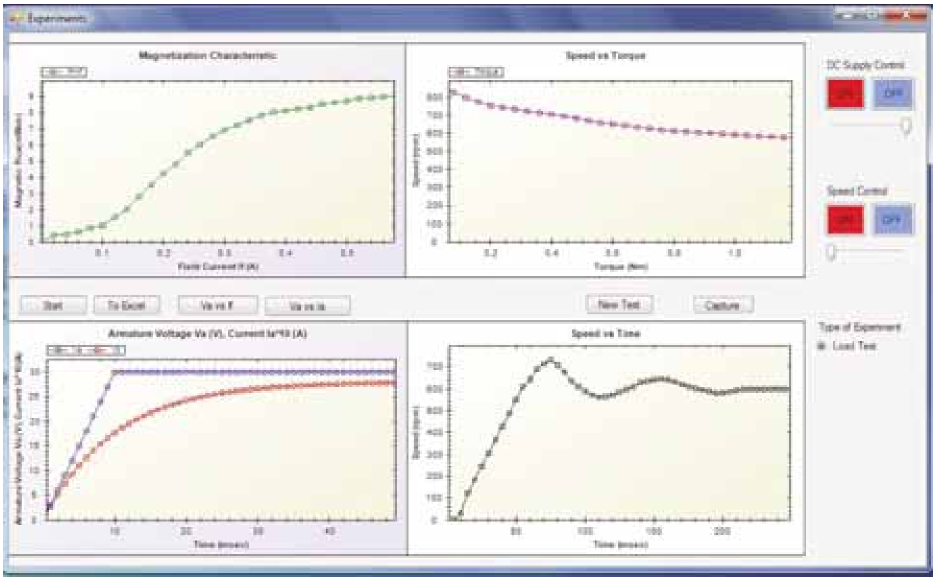

with improved specifications. Key features of the AD629 amplifier can be summarized as:

- ±270V Common-Mode range;
- ±500V Common and Differential Mode input protection;
- Wide Power Supply range up to ±18V.

The isolator amplifier of the AD629, shown in **Figure 4**, operates as a differential to single-ended converter amplifier with a simple gain of 1, where the amplifier output voltage is $V_o = R_1 I_1$.

The output voltage of the isolation amplifier is bi-polar, however, the analogue input of the microcontroller, which converts the analogue data into digital, can only accept input voltages between 0-5V. To get maximum resolution from the A/D converter, the bi-polar voltage is converted from ±0.5V to 0-5V as follows.

The measured signal is amplified by a factor of 10 in the first stage so that the measured range of ±0.5V is increased to ±5V. In the second stage, this signal is averaged with 5V by using a simple two-resistor averaging circuit. The relationship between the amplifier output voltage and the voltage applied to the A/D converter can be written as:

$$V_{ad} = (10xV_{out} + 5) / 2 \qquad (1)$$

The second op-amp in Figure 4 acts as a 1-1 buffer to the A/D input, and the output of the buffer circuit is filtered using a passive RC filter just before it is applied to the A/D stage.

The results are:

- +5A at the input of the current channel is represented by 5V at the input of the A/D;
- 0A at the input of the current channel is represented by 2.5V at the input of the A/D;
- -5A at the input of the current channel is represented by 0V at the input of the A/D; where the intermediate values are linearly dependent.

Voltage Channels

There are 3 independent voltage input channels on the DAQ Card whose measurement range is ±15V. The structure of the voltage channel circuit is very similar to that of the current channels presented in Figure 4 while the differences are as follows:

- Instead of routing the current through a sensor resistor, the input voltage is directly routed to the input of the High Common-Mode Amplifier, AD629.
- The multiplication x 10 is not needed in the voltage channel circuit where the input voltage is already higher than the measurement range of the voltage channel. Instead, a simple voltage divider is used to reduce the input voltage to a reasonable level.

Inter-channel isolation is achieved using the same principle as in the Current Channels using the isolation feature of the AD629.

Hall Sense/Auxiliary Analogue Input Channel

This channel is a simple general purpose single-ended A/D input which may be used to measure the magnetic flux or the speed

Figure 6: *Animation: Induction of 3-phase voltages in a synchronous generator*

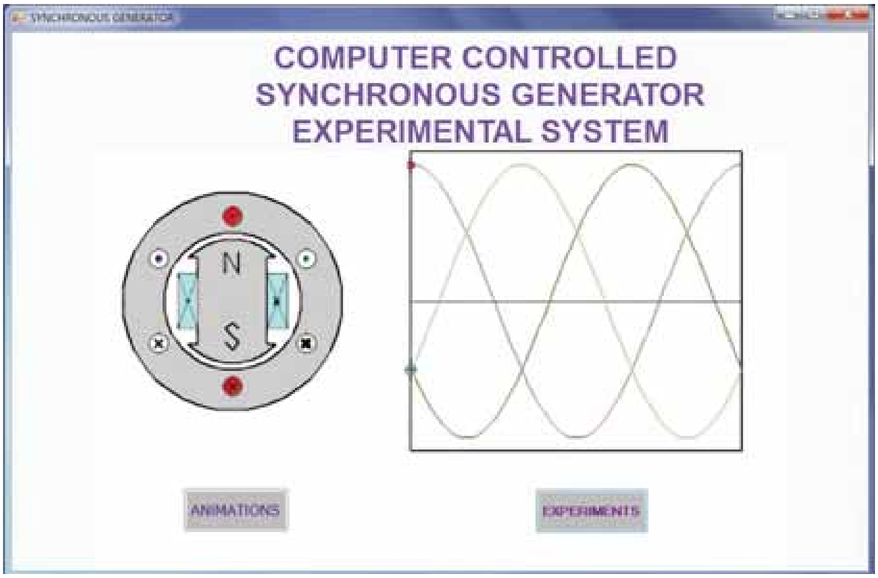

in electromagnetic and electromechanical devices such as transformers, motors and generators. As the measured variables are inherently isolated, there is no isolation requirement for this channel where the maximum input range is ±5V. Only the last two stages of the circuit of Figure 4 are used in the Hall Sense channel.

Smart Display of Test Results

Figure 5 illustrates the display format of the SEMS showing the experimental results of a 75W, 30V, 600rpm compound-wound DC motor which is initiated with a soft start. The type of the test can be selected on the user interface, where currently the load test is selected. Transient variations of the armature voltage and current and of the rotor speed are displayed on the bottom two charts over the initial starting period under full load. The load torque was then changed from full load to no load to obtain the speed versus torque characteristic curve which was displayed on the top right chart of **Figure 6**. It is possible to display the experimental data such as the voltage (V), current (I), torque (T) and speed (n) on 4 different charts simultaneously. In each chart, variation of measured data can either be plotted with respect to time (t) as shown in the bottom two charts or the characteristic relationships such as the magnetic flux (Φ_f) versus the field current (I_f) or T versus n curves can be monitored as illustrated in the top two charts. Switching from n versus t and T versus t curves to the n versus t curve is realized by a simple click on the related function button on the user interface.

The measured values at each sampling point can be displayed by selecting the *Show Point Values* entity with a right mouse click on the chart. The time axes can be expanded or contracted to display the regions of interest more clearly, simply by highlighting the region of interest with the mouse. All plotted data points can be tabulated in Excel format by clicking the TO EXCEL button on the menu.

The axes are adjusted automatically, as the magnitude of the input data changes, to display the measured data with the best resolution, the time axis is also adjusted dynamically according to the time elapsed during measurement. This allows a better display of transient as well as steady-state behaviour of the electrical system under test. The labels and the units of the axis on the charts are automatically set according to the experimental configuration selected by the user. Open source software called ZedGraph (**www.zedgraph.com**) was used to achieve these versatile chart display features.

The DAQ card of the SEMS is bi-directional in operation and can not only receive signals from the experimental system, but also enables the control of input control variables. For example, the supply voltage or the speed of the motor can be controlled with manual software controls on the menu via the mouse.

The user can easily configure the user interface of the management software by entering the DAQ input and output control and display features of the new experiment via a configuration routine. For expert users, SEMS provides an API of the DAQ card which allows them to write an application specific code in C#, or Delphi to introduce more sophisticated control or display features to their experimental procedures.

Figure 6 shows an example of an animation to illustrate the principles of induction of 3-phase voltages in a 3-phase synchronous generator, where the generation of 3-phase voltages which are displaced by 120 degrees can be traced easily by controlling the motion of the rotor manually. This enables the student to grasp the reason why a phase difference of 120 degrees occurs between 3-phase voltages as the rotor rotates, which is not easily explained by drawing the cross-sectional view of the generator and the voltage waveforms on a blackboard.

Intelligent Data Collection

An intelligent experimental data collection, analysis, monitoring and control system has been designed and implemented successfully. The new system helps the instructor and the student to perform experimental work in a digital environment, where all measured data can be monitored on an LCD display and stored in memory for further processing.

Characteristic curves and tables can be easily produced, analyzed and reported in the digital environment of the SEMS. Transient as well as steady state measurements can be stored and displayed on the same graph. This allows the student more time and a friendly user interface to develop new experimental procedures and to get an in-depth understanding of the operational features of electrical and electronic circuits and systems.

New software modules are being developed for the SEMS to include pop-up questions and quizzes to help the student to prepare for the experimental work and also to let the instructor evaluate the performance of the students interactively and automatically, thus eliminating the overheads of instructor evaluation.

Networking among the SEMSs in a laboratory is also possible, where data flow between instructor and students can be provided in both directions. This will enable the instructor to check the performance of the students and guide them interactively. ■

Revolutionary 3D Filter For Audio, Satellites, Cars, Medical Devices & INDUSTRIAL MEASUREMENT

Clemens Par, founder of Swiss high-tech start-up swissaudec, explains how a mathematical filter, named VoiCode, makes the unachievable in professional audio very easy

IT ALL STARTED when the British engineer Alan Dower Blumlein and his wife went to the cinema and everybody was still used to one channel based mono audio signals. While the protagonists were moving on the screen, dialogues seemed to be frozen in one spot. Blumlein – who had joined Columbia Graphophone in 1929 (which in 1931 became EMI) – stated after the film that he had found a solution how to render audio information in a spatial manner. Blumlein and EMI filed a patent on December 14, 1931, entitled Improvements in and relating to Sound-transmission, Sound-recording and Sound-reproducing Systems. Stereo was born!

However, it would take another 27 years till the first commercial Stereo LP records would be found on the market. Blumlein, who had just started his career as one of the most productive British inventors (from 1927 onwards he was author of 128 patents), was never to see the commercialized version of his ideas. He died in a plane crash in 1942 when testing the radar system H2S designed for the RAF. Blumlein's reputation for many years seemed to have been in this field.

Major Acheivements

Stereo – being one of the main achievements in electroacoustics – turned out to be a major economic failure within the granted time of patent protection, and it may be a historical lesson for the enormous difficulties which a new technology may face, despite its final tremendous social and economic impact.

In the fifties Bell Laboratories started a research activity in the field of so-called 'pseudostereophonic' signals. Manfred R. Schroeder, a German physicist then suggested to generate a sum and a difference signal out of a single mono channel signal the way that their sum equals 1 (the original mono signal would then be rendered). Most prior art 'pseudostereo' methods are more or less based on such a processing method, however, they fail to render plural sound sources constantly on the sound stage as these sound sources would move in functional dependency on frequency.

Figure 1: Recording a big symphony orchestra with one single mono microphone in full Stereo or surround seemed to be impossible so far. A mathematical filter, named VoiCode, finally achieves this goal on a professional level

[Image © Jason Cohn]

The British mathematician Michael A. Gerzon, a professor at Oxford University, who by his love for music and electroacoustics was to be the most eminent figure in theoretical electroacoustics (inventing together with Peter G. Craven a three-dimensional sound recording system named the 'Soundfield' microphone), suggested a cascaded complex gain processing peudostereophonic method as well as a frequency-dependant rotation matrix in order to stabilize this undesired movement, which implies that plural recorded sound sources rendered by the same mono signal will be uniformly dispersed across the sound stage.

Pseudostereophonics methods, therefore, proved themselves inferior to classical stereo recording techniques so far and never enjoyed vast popularity among engineers and amateurs.

Different Approach

When starting my own research activities in this field trying to develop a mathematical filtering method, which then should work in line with pressure zone microphones in order to render fully professional stereo or multi-channel sound, I was not driven by the agnostic approach scientists had already adopted when talking about pseudostereophony. All attempts had been arbitrary so far, and none of these

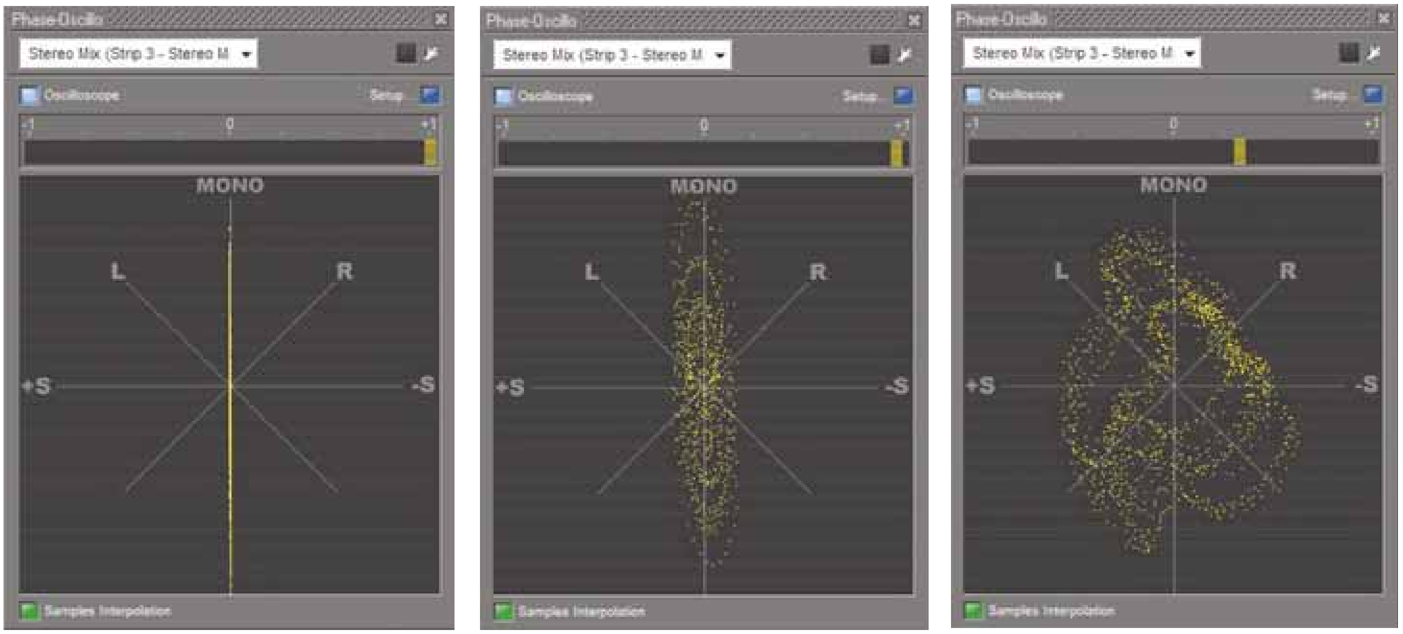

Figure 2: *A mono, prior art pseudostereo and VoiCode signal shown on a goniometer. With VoiCode the spatial distribution of plural sound sources across the sound stage can clearly be seen on the screen*

pseudostereophonic methods ever had taken the original recording situation into consideration.

MS recordings techniques, still on the basis of PZM microphones, immediately captured my interest. At that time I had plenty of studio experience working for all major broadcasting corporations in the German-speaking countries and was about to establish my own recording studio. When it came to the acquisition of professional condenser microphones I asked myself the question how much of these microphones I would need at minimum.

The first rudiments of my invention were layed down the same evening: I had found the first pseudostereophonic filtering method that would render plural sound sources varyingly distributed in space, without their moving in functional dependency on frequency!

The Eureka! moment would take some time as I still had to establish my studio in order to prove my theories – which after the first success with an analogue-digital prototype underwent its metamorphosis – until it finally turned out to be a highly elaborate one-channel based audio lab.

From 2007 onwards the first rudimentary filters were turned into highly elaborate audio systems; I filed seven patent applications on an international scale.

MS recording techniques in many ways show similarities to Schroeder's initial attempts. They all use a mid microphone signal M and a side signal S which is principally a figure-eight pattern microphone turned 90 degrees to the left. A stereo representation then is calculated by the following equations:

(1) $$L = (M + S) * 1/\mathrm{sqrt}(2)$$

(2) $$R = (M - S) * 1/\mathrm{sqrt}(2)$$

which imply that the sum of the left and the right channel represent the mid microphone signal M – as would be with Schroeder's system.

Unlike Schroeder who arbitrarily distributed frequencies to the left and the right channel by means of complementary all-pass filters, I focused on the question whether an S signal could be interpolated from the original recording situation and at the same would solve Gerzon's problem of plural uniformly dispersed sound sources.

Angular spread immediately turned out to be the major factor and, indeed, the angle-dependant simulation of plural omnidirectional microphones that would replace the initial figure-eight pattern microphone proved to be successful in reconstructing a spatial sound image.

What the system would calculate in detail were specific delays and amplitude corrections with respect to the angular spread of sound sources by which the entire spatial information could be recovered. Simple in its structure the core of this technology showed additional parameters for optimizing the sound stage. The final result: The spatial distribution of sound sources would be absolutely respected by such a system.

Major Breakthrough

The first pratical results represented a major breakthrough in electroacoustic filtering; they

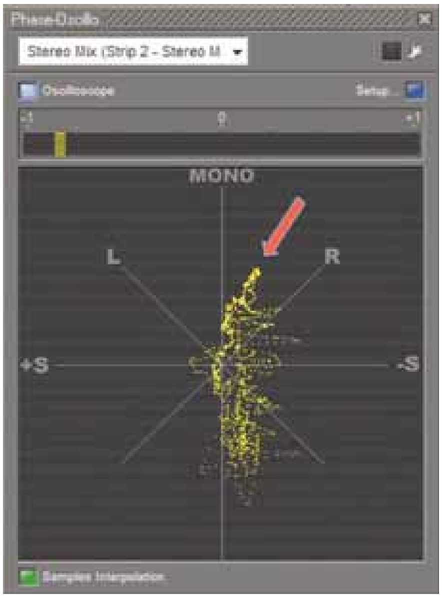

Figure 3: *Localization of a mechanical loudspeaker defect by means of one single mono test microphone and VoiCode. On the goniometer the defect is mapped top right (marked by an arrow)*

Figure 4: *Graphic interface of Merging Technologies's Digital Audio Workstation Pyramix with the inserted filter prototype [Image © Merging Technologies]*

would show no difference in quality when being compared to first-rate professional MS recordings.

These new filters could be adjusted the way that a specific degree of correlation could be obtained, literally varying from -1 to +1. They would show distinct plural sound sources on the sound stage that would no more shift in functional dependency on frequency.

However, what about existing recordings without any information about the angular spread of sound sources? Let's, for instance, consider a jazz recording from the fifties. No photographs, no written records, not the slightest clue how this recording came into being, just one single microphone signal or the sum of several mono microphone signals magnetized on wire, wax, tape or shellack etc.

MS recording techniques, as are interpolated with the present filters, show vast editing possibilities. For instance the sound stage can be varied by changing the amplitude of the figure-eight S signal. The same variation, on a different mathematical basis, is also possible with the present filters.

By employing statistical methods we have made these filters "intelligent", which now will reconstruct the missing angular information for a genuine MS representation by calculating the 'best case'; according to the principle that if an interpolation method equals the interpolated method the "best case" represents the correct parametrization which will "reveal" this formerly hidden angular spread.

This feature is of particular importance for deficient MPEG satellite signals that run a mid channel (L + R)/2 and a side channel (L – R)/2, which are similar in their structure to MS signals (see above). Such deficient satellite signals may occur with so-called "rain fade" – meteorologically induced incoherent signal transmission. When applying our filters in this field the primary focus is to reconstruct the mid channel signal and to gather as much information about the side channel as possible – before processing the final signal as outlined above. The result is a fully professional stereo or surround signal despite "rain fade".

The same is valid for hybrid Internet radio, DAB, FM and PC streaming chips. FM radio broadcasts to a very large degree (for instance in the United States and abroad) are still mono broadcasts, which by means of our system may be easily converted to genuine stereo or surround.

Revolutionizing Consumer Electronics

Electronics are reigned by the principle of perpetual miniaturization and transducers are fully in line with this fact. Only a few years ago MEMS (Micro-Electro-Mechanical Systems) started to enjoy wide popularity among electronic device manufacturers, and the first MEMS microphones were built into consumer electronics due to their indifference to electromagnetic fields. Some 1.7 billion of these miniature microphones, which are directly mounted on a tiny chip, have globally been sold, so far. They generally show an omnidirectional polar pattern and, therefore, can only be used with highly instable prior art A-B stereophony.

Their frequency response, however, is excellent, and together with the present filters (for which we have chosen the portmanteau VoiCode in commemoration of Alan M. Turing's and Homer W. Dudley's scientific contributions to SIGSALY, a crytographic audio filter used by the United States during World War II) can be turned into fully professional stereo or surround microphones that will, for instance, fit into an ordinary computer, handycam, mobile phone or iPod.

A fully professional recording studio always at the user's fingertip might be the consequence (as our VoiCode filter layouts only consume about 1% of the surface of an average consumer electronics microcontroller, they may likewise be directly integrated on the MEMS microphone's chip and may further revolutionize miniature consumer electronics).

The spatialization of sound is a very important feature with handsfree sets, particularly in the automotive industry. As the car's noise suppresses important formant frequencies and consonants like "b", "p", "g", "k", "d", "t" or "f", "s" cannot be discerned any more, the driver (in his attempt to catch the important information) is distracted. He will furthermore focus on the localization of his interlocutors in one single spot somewhere between the car's loudspeakers.

The smart answer to this dilemma is to create a stereo or surround sound image out of the original phone signal by means of VoiCode. This new feature could be in line with further VoiCode filtering of deficient car FM radio signals which is based on the same technological background as the reconstruction of satellite broadcasting signals in case of "rain fade".

Conventional car FM stereo signals furthermore suffer from the fact of continuously changing receiving conditions. As soon as the sub-channel L – R is poor the radio receiver automatically switches to the main channel L + R, which leads to an incoherent sound image that may be described as "stereo pumping"; this will not occus with VoiCode.

Calculating MS Stereophony

The present method to calculate an MS stereophony on the basis of an angle-dependant simulation of plural omnidirectional microphones has also successfully been tested in industrial measurement techniques: by means of VoiCode filtering we then could localize sound sources or reflexions with one single mono microphone; in our case mechanical loudspeaker defects which had been recorded by one single omnidirectional test microphone. These mechanical defects indeed could be made visible with a goniometer (as their localization is frequency-invariant).

The same methodology may likewise have a strong impact in related fields – stabilizing, for instance, medical Live 3D ultrasound (which currently is based on an about-turn of the scanning plane) and hand-carried ultrasound – as angular sound reflections may now be localized by our VoiCode filters. Hearing aids may be further miniaturized, as no second microphone is needed to calculate the precise localization of sound sources.

The present system is subject matter to an industrial research and development project with Ecole Polytechnique Fédérale de Lausanne (EPFL), the Swiss centre of excellence in electroacoustics. We are currently preparing our first industrial pilots in the field of MEMS microphones, the automotive industry, FM radio and industrial measurement techniques.

Sound Alternative

In the long run, the VoiCode technology might be the sound alternative for creating and decoding stereo or surround – just a handful filter parameters of a few bits then would be lingua universalis in modern electroacoustics – replacing the current bulky multi-channel formats.

However, that a mere mathematical filter together with one single mono microphone would record a big symphony orchestra in perfect stereo or surround even perplexed me when I ran my first implementation. Since then, practical experience and the multitude of fascinated individuals have showed me the way to numerous industrial applications. ■

LCD Television DEMYSTIFIED Part 1

Fawzi Ibrahim, a former lecturer and author of several books including Newness Guide to Television and Video Technology, gives a practical overview of LCD television receivers. In this part, Ibrahim explores the modular structure of these receivers, identifying the individual boards and explaining their functions

TRADITIONALLY, TAKING the back off electronic products is something many engineers would be happy to do. With flat screen televisions however, this has not always been the case. Even experienced engineers are reluctant to open up a modern LCD television not to mention an amateur or an enthusiast.

These sets seem to have acquired an underserved mystery. In this two-part article, I will attempt to demystify LCD television receivers to show that, if anything, there has never been a better or more productive time to explore the inner 'bowels' of these products. Part one will explore the modular structure of these receivers, identifying the individual boards, explaining their functions and their inter relations. In part two, we will take the back off a typical receiver, identify each board, connector and cable and put together testing and fault-finding pointers.

The high level of integration coupled with the difficulty of obtaining service manuals with detailed schematic diagrams, make component-level fault-finding problematic to say the least. Apart from the speculative replacement of the usual suspects in a power supply unit (large smoothing electrostatic capacitors and power components) and the odd dry joint, fault-finding is generally restricted to board-level diagnosis and replacement. The first step in this endeavour is to identify the faulty board, something that can be greatly simplified with the use of a main PCB simulator as we shall see in the second part of this article.

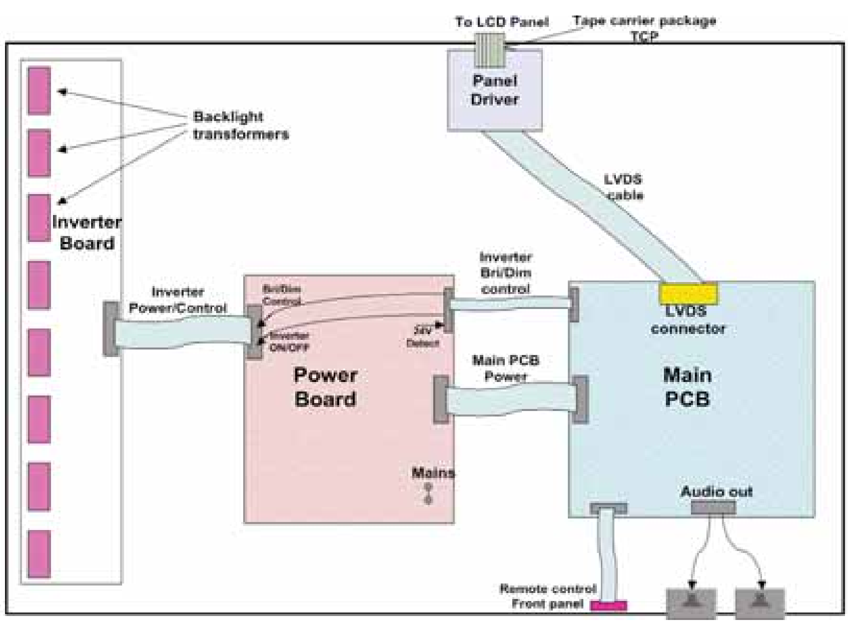

Figure 1: *Board schematic of an LCD television receiver*

Board-Level Schematic

LCD television receivers consist of two principal boards: the power supply board and the video/audio/control PCB, commonly known as the main board or small signal board (SSB), illustrated in **Figure 1**.

The main PCB carries out all necessary control and signal/data processing for good quality picture and sound reproduction. The receiver contains two other PCBs: the inverter (shown on the left) to drives the backlight fluorescent tubes and the LCD panel driver/scanner, also known as T-Con (timing and control) board which feeds the video data to individual pixels as the screen is scanned.

Some receivers have two inverters, one on each side of receiver. For small-size televisions, less than 32 inches, the power requirements of the backlight are such that the inverter may be incorporated within the power supply board itself.

When the set is plugged into the mains, it goes into the standby mode, normally indicated by a red LED on the front. The power supply is turned on, an event usually accompanied by one or two soft clicks, by a signal from the main PCB. The power supply generates a number of voltages: typically 3.3V, 5.3V and12V for the main PCB and 24Vfor the inverter. The actual voltages generated by the power supply

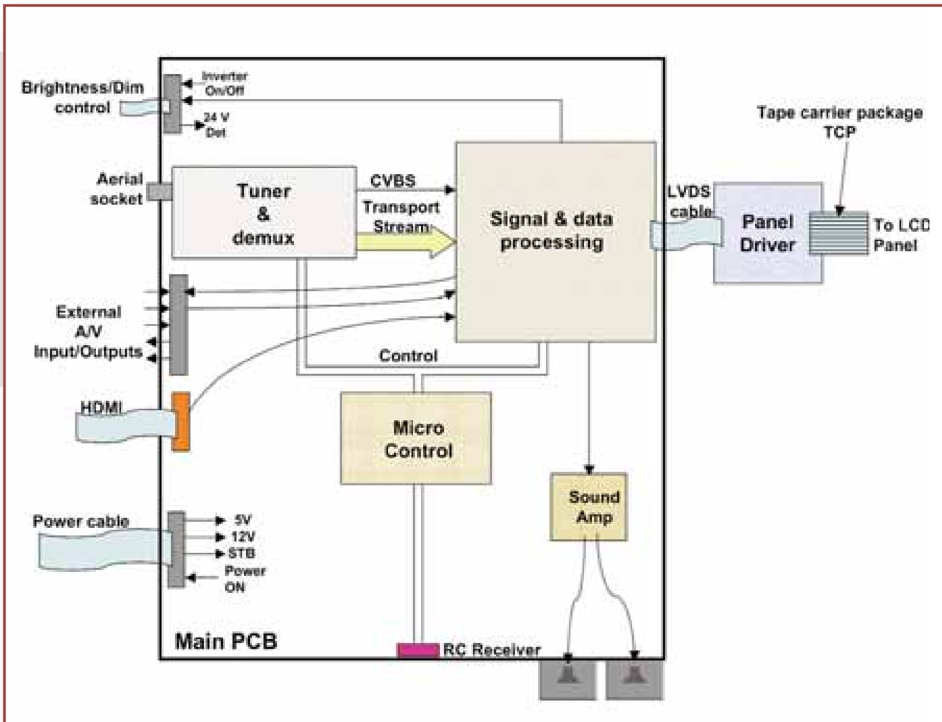

Figure 2: *Principal elements of a Main PCB of an LCD television receiver*

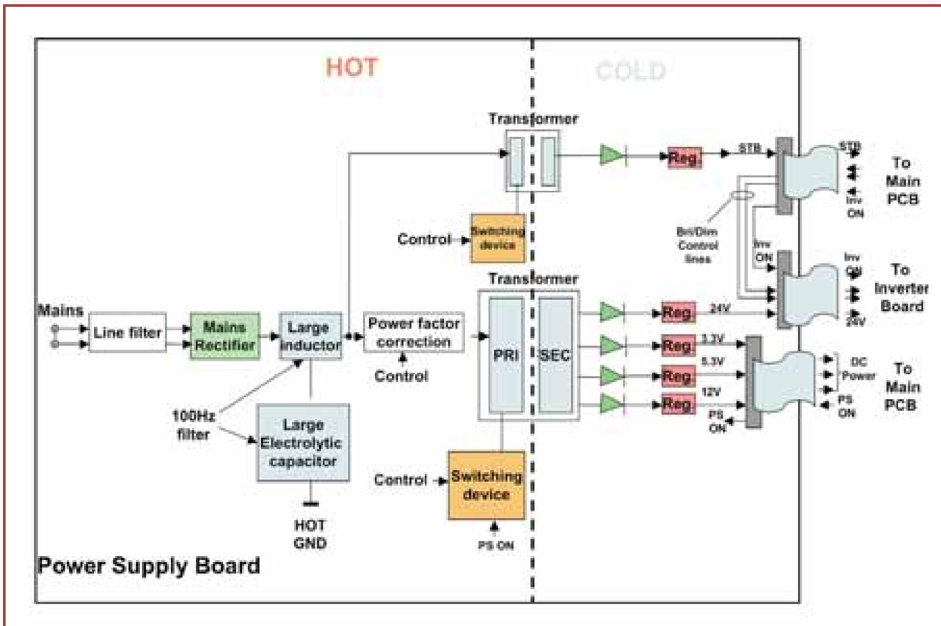

Figure 3: *Recognizable elements of a Power Supply Board of an LCD television receiver*

differ depending on the make of the receiver.

After processing the incoming signals, video data are forwarded to the T-Con board via the LVDS cable on its way to the LCD panel for picture reproduction. Sound is sent to the loudspeakers following appropriate amplification. The LVDS cable also carries DC power and other control lines necessary for the operation of the panel driver/scanner. As the video flow continues, it is tracked by the main board and assessed for its brightness and content in order to control the brightness of the backlight tubes on the one hand and the transmissiveness of the LC cells on the other, frame by frame, a process known as adaptive transmissive scaling (see box). Signals for backlight brightness/dimming control from the main board are sent via the Bri/Dim control cable to the power unit on its way to the inverter board via the inverter power/control cable. Control signals for the transmissiveness of the LC cells are sent to the panel via the LVDS cable.

The Video/Audio/Control Main PCB

The main board is responsible for the processing of video and audio signals, as well as the control of the system in general. System control is carried out by a microprocessor and associated memory using one or more serial control bus structure such as I2C. Incoming A/V signals may take the form of terrestrial or satellite modulated radio frequency broadcasts, analogue A/V via an external port (SCART, component video, CVBS and associated L/R audio), digital A/V (via the HDMI port) or digital audio (via Sony/Philips interface format, SPDIF).

Modulated RF signals arrive at the tuner via a terrestrial (Freeview) aerial or a satellite dish. Unlike satellite television which is fully digital, terrestrial television continues to broadcast analogue as well as digital channels. For this reason, terrestrial receivers use a hybrid integrated tuner which can demodulate analogue as well as digital broadcasts to produce CVBS and sound IF (SIF) for the former and an 8-bit transport stream for the latter (see box). In older sets, and in this the fast evolving technology, sets made more than four years ago come under the category of 'old', two separate tuners are used, one for analogue and another for digital channels.

The transport stream produced by the tuner consists of the video, audio and control packetised elementary streams (PESs) that belong to a number of programmes sharing one terrestrial 8-MHZ channel. The PESs of the selected programme are picked up by the demultiplexer within the processing unit. As for external audiovisual signals (analogue and digital), they are fed directly to the processing unit. The processing unit carries out all necessary video and audio processing functions including audio and video decoding, image formatting and scaling to produce LVDS-compatible video

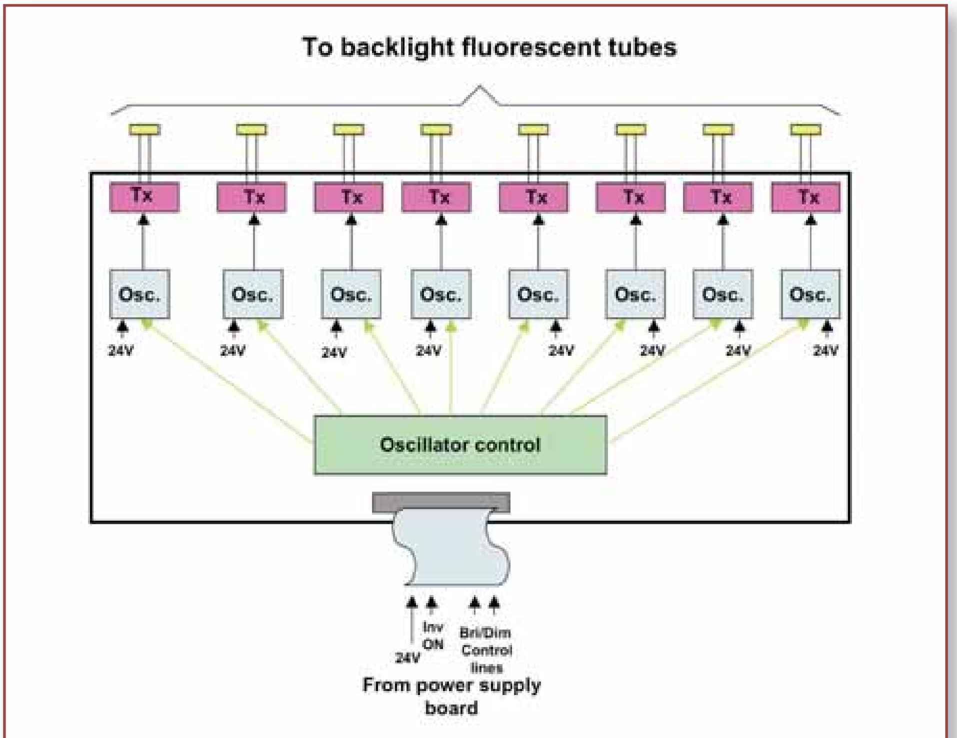

Figure 4: Main elements of an inverter board of an LCD television receiver

data and suitable stereo audio signals as well as other analogue and digital signals for external outputs. Decoding is normally restricted to MPEG-2 standard definition (SD) video. However, some terrestrial TV manufacturers, in anticipation of high definition television (HDTV) terrestrial broadcasts, have included high definition MPEG-4 decoding capability. Terrestrial HD channels are now available on Freeview in some areas in the UK which could be received if you have one of those receivers. Such capabilities are surprisingly not sufficiently publicised but certainly worth taking into account when purchasing a television receiver. Such capabilities are surprisingly not publicised but worth taking into account when purchasing a television receiver.

The Power Supply Board

Figure 3 shows the most recognizable components of a typical power supply board, recognisable by their size and in the case of power transistors and diodes, by their heat sinks as well. The power supply is of the switched-mode type to reduce size and improve efficiency. Mains 250V AC is fed into a full-wave mains' rectifier through a line filter. The resulting DC (in the range of 350V) is then smoothed by a 100Hz filter, consisting of a large inductor and a big electrolytic capacitor.

For LCD panels of 32 inch or over, a power factor correction circuit is normally introduced at this point, with the purpose to improve the power factor of the television receiver by reducing its reactive load current. The PFC unit consists of a switching element not dissimilar to the main switching element that follows. The main components of the switched-mode power supply, is a switching device, usually a power MOSFET mounted on a heat sink and a large output transformer that straddles the Hot and Cold sections of the power board.

The switching element chops the DC at a frequency of 10kHz or above. The chopped DC is picked up by the secondary windings of the transformer, rectified, smoothed by the use of an RC filter (not shown) and regulated to provide voltages for the main PCB board (typically 3.3V, 5.3V, 12V) and 24V for the backlight inverter.

The standby voltage is generated separately with its own rectifier, switching element, transformer, which also straddles the hot/cold barrier, rectifier, smoothing circuit and regulator. The standby voltage, STB is fed to the main PCB to keep the remote control unit alive so long as mains power is connected to the receiver. When the TV is turned on, the main SMPS turns on to generate the various DC voltages. The 3.3V, 5.3V and 12V supplies are fed to the main PCB booting up the microprocessor and initialising the other programmable chips ready to commence processing.

The Inverter Board

The purpose of the inverter board is to convert the 24V DC from the power supply into a 50-60kHz sine wave that is needed to drive the fluorescent tubes. The sine wave has an amplitude in the region of 3000V and may be picked by an oscilloscope by simply placing the probe on an oscilloscope in the vicinity of the transformer. The actual DC-AC conversion is carried out by a number of tuned oscillators coupled to high turns-ratio transformers ensuring a secondary voltage of few thousand volts. The main elements of an inverter board are shown in **Figure 4**.

The brightness of the tubes may be set through the available options in the receiver's menu listings to suit users' preferences. It may also be varied, in real time by the Bri/Dim controls to reflect the contents of the picture in receivers using transmissive scaling techniques. The oscillators are enabled by a signal from the main board and are designed to turn off if one or more tubes fail to light up.

The Panel's Scanner and Driver

Also called T-con, the LCD panel's scanner/driver receives coded digitised video information from the main board together with DC power and control lines such as clock, Bri/Dim and other instructions via the LVDS cable. It scans the panel, line by line while the cells along each line are address and their luminance levels set by an analogue voltage fed down vertical data columns. The overall transmissiveness of the cells is varied in real time by the Bri/Dim control signals. ■

This article continues in the next issue of Electronics World magazine.

USB Conversion of Serial and PARALLEL DEVICES

John Hyde from Future Technology Devices International (FTDI) will implement a series of USB projects over the course of the following editions of Electronics World. This first example concerns the USB conversion of legacy serial and parallel devices

Figure 1: Representative serial device

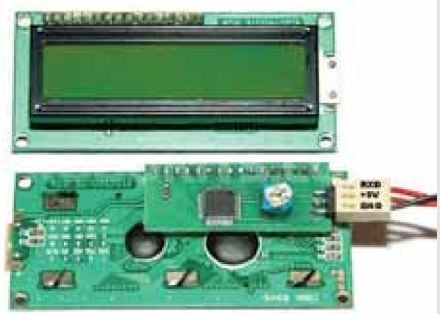

THE EMBEDDED WORLD still favours serial ports because they are easy. A serial port has just two data wires, TX and RX, for full duplex communications, plus a reference ground wire. Serial ports became popular with the introduction of modems in 1977 and the RS-232 standard also includes modem control signals such as DataSetReady and DataTerminalReady. Signalling levels are ±12V, which tends to limit the maximum data rate to 56 Kbaud. Once both ends of the wire agree on the baud rate it is a simple matter of sending/receiving any stream of data bytes.

Unfortunately, the simplicity of exchanging data streams is also the serial port's Achilles Heel. Most serial links also need to exchange some control information. This is embedded in the data stream using some kind of escape sequence. This, by itself, is not a bad technique; the issue is that there is no standard escape sequence, resulting in applications software being tied to a specific piece of hardware. Also there is no standard way for application software to identify attached hardware.

The real problem, however, comes when attaching a serial device to a PC only to discover there are no serial ports available. PC hardware changes at a quicker rate than typical embedded systems and, in order to take advantage of 'PC economics', we need to follow their trend.

Figure 2: Connecting the TTL-232R cable to the serial display

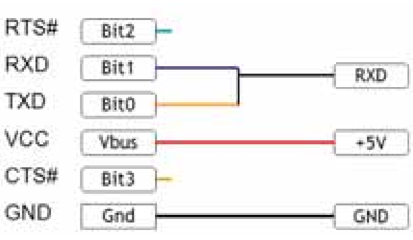

PC software has also changed dramatically. Early PCs had their internal hardware exposed via BIOS listings. You were actually encouraged to access the serial ports at 0x3F8 and 0x2F8. This all changed with the introduction of 'protected mode' Windows, where applications software was prevented from accessing the physical hardware. The same is true today for Mac OS X and Linux. All three OSs support multi-tasking and multi-applications; they must own the underlying computer hardware so that they can manage its use. The impact for embedded developer is that serial ports must be accessed via a device driver – COMxx for Windows, while in Mac OS X and Linux this is /dev/tty. Once you encourage the OS to supply a 'handle' to a serial port then it is possible to read and write data streams with the serial port.

Let's look at an example of converting a typical serial device to a USB device. The display shown in **Figure 1** has a 2 line x 16 character format that accepts ASCII characters through a 9600 baud serial connection. Non-displaying characters (0x00..0x1F and 0x80..0xFF) are interpreted by the on-board microcontroller to implement special functions such as the set-up and display of custom characters and turning the backlight on/off. It only needs a single IO pin to drive the display.

Rather than creating a custom example program, I use software for the PC that is already available and designed to support serial ports. For the Windows PC we can use HyperTerminal and for the Mac/Linux PC we can use CoolTerm. Utilising a USB-to-Serial cable from FTDI, the TTL-232R and its drivers, first connect the non-USB end of the cable to the display as shown in **Figure 2**. The cable provides power to the display and here we have looped TXD back to RXD.

The FTDI drivers have two distinct interfaces, D2XX which we use to access low level functions and VCP, a Virtual Com Port interface. The Windows driver supports both interfaces in a single installation, but only one may be used at a time. Insert the TTL-232R cable into the PC and then display the hardware configuration using the Device Manager in the system control panel. The configuration is shown in **Figure 3** and note that the cable enumerated as a COM port.

Spin up HyperTerminal in the accessories directory and select the COM port assigned to the TTL-232R cable. Now jump to the 'Configure the terminal program' section.

For a Mac, operation is a little trickier, since the FTDI drivers are not combined. Both the D2XX driver and VCP driver need to be installed. Decompress the FTDIUSBSerialDriver.dmg file downloaded from FTDI's website, click on FTDIUSBSerialDriver package and follow the installation instructions. Insert the TTL-232R into the PC and the OS will preferentially choose the VCP driver. **Figure 4** shows the output of the System Profiler tool and lists the FTDI cable connected to USB. Next, spin up CoolTerm and select the usbserial device.

Configure the Terminal Program

Choose 9600 baud and open a connection. Type "Hello World" then note that this also appears on the 2-line display. USB is embedded so deeply that we haven't needed to be exposed to any USB at all. All of the USB aspects have been handled by the FTDI cable and its VCP driver.

So conversion of a serial device to a USB device is relatively easy to accomplish, all the hard work being carried out by the OS and its drivers. They handle the differences in hardware and we, at the application program level, need not be concerned about exactly how this is done.

Switching Back to the D2XX Driver

The D2XX driver is always available to Windows users so you may skip this section. The Mac OS X user can temporarily or permanently remove the VCP driver using the Terminal application and view the system extensions to identify the system name of the FTDI cable:

```
cd /System/Library/Extensions
ls
```

You can remove it for the current session with:

```
sudo kextunload FTDIUSBSerialDriver.kext
```

To permanently remove it (which will mean reinstalling the package if using the VCP driver again) use:

```
su
rm –R FTDIUSBSerialDriver.kext
```

Optimising the Serial Connection

Now, let us look at a few optimizing steps. The serial display is not typical as it used TTL levels rather than RS-232 voltage levels. The top of **Figure 5** shows a more common serial device. It has an internal microprocessor/microcontroller driving an RS-232 voltage converter for PC communications and drives custom IO, specific to the embedded application.

In the centre of Figure 5 I have replaced the serial cable with the FTDI TTL-232R cable. This drives TTL levels so there is no need for the RS232 voltage converters. We have a problem with the connector, however, since the industry expects RS-232 voltage levels on the 9 pin (or 25 pin) serial connector. We shall deal with this issue in a moment.

Now look at the third diagram in Figure 5: I have moved the FT232R part from the PC end of the cable to the device end. This FT232R replaces the RS-232 voltage converter and I replace the serial port connector with a USB B connector (standard size or mini-B). This means a standard USB cable can be used to connect the new device to the PC. Another advantage of having the FT232R at the device-end is that you have access to all 12 IO lines.

So we have migrated a serial device into a USB device. In addition, if needed, we could increase the baud rate to the device. Standard serial cables easily support 56 Kbaud and some 192 Kbaud while the USB connection can run up to 3 Mbaud. A USB cable can also supply up to 500mA at 5V. If the target device can operate at or below this level then it is possible to eliminate its power source and thus reduce manufacturing costs.

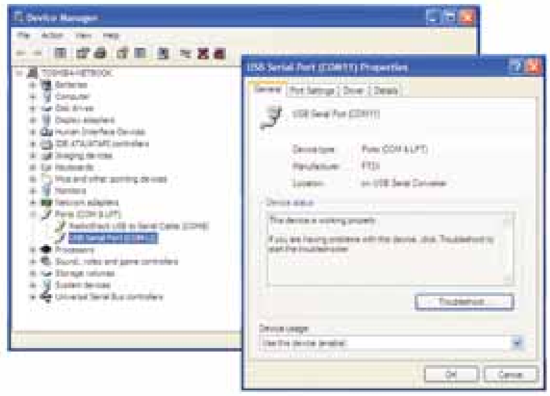

***Figure 3:** USB cable recognised by Windows as a COM port*

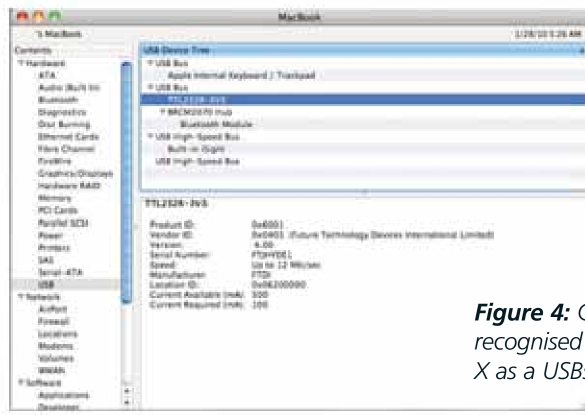

***Figure 4:** Cable recognised by Mac OS X as a USBserial device*

Converting a Parallel Device to USB

A companion part to the FT232R, the FT245R replaces the serial interface with a parallel bi-directional FIFO interface for higher data throughput rates. Converting a parallel interface device to a USB device follows the same methodology as the serial device. From an applications software perspective you still treat it as a serial port but, otherwise, the software is unchanged. You can exploit higher speeds and USB-provided power.

By using the VCP driver it is possible to present the USB device as a COM port. While this is convenient as a transition strategy it does not address the serial port's main weakness, that of device identification. If you have multiple devices and chose the wrong COM port number then your application software will fail. I would, therefore, recommend using the VCP driver as an initial step, but migrating to D2XX in the longer term since it has more capabilities. ■

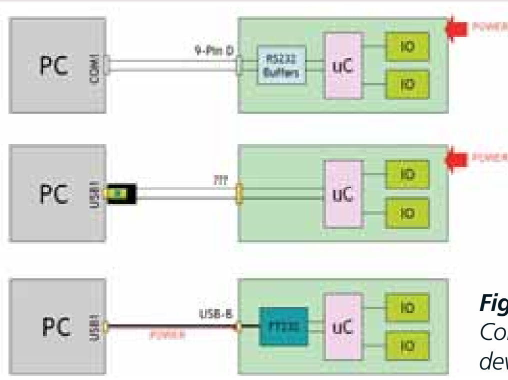

***Figure 5:** Converting a serial device*

HMP2000 SERIES – UNIVERSAL APPLICATIONS EXTENDED

The HMP2000 series High Power Supplies were improved by adding an important feature: Channel 2, so far an auxiliary channel with 0-5.5V was upgraded to a full-grown 0-32V channel. This improves the univeral applicability significantly, also with regard to future presently unknown applications.

The HMP2020 now features two identical channels with 0-32V, one delivers 10A, the other 5A. The HMP2030 now has three identical channels with 0-32V/0-5A. Also new are the LabView, CVI and plug-and-play drivers for all types of the HMP series that also includes the HMP4030 with its three and the HMP4040 with its four identical 0-32V/0-10A channels. Hence, all programming systems and interfaces (USB, LAN, IEEE, and RS-232) popular in the ATE world are now being supported. The drivers are available at no cost for downloading from Hameg's website.

www.hameg.com

HIGH-PRECISION VERSION OF THE WORLD'S SMALLEST DIGITAL HUMIDITY SENSOR

Sensirion has launched a high-precision version for applications with stringent accuracy requirements – the SHT25 which precisely measures relative humidity over a range of 0 to 100% RH and temperature over a range of -40 to +125°C.

The sensor achieves a typical accuracy of 1.8% RH (at 25°C) for relative humidity and ±0.2°C for temperature. For both quantities, the typical tolerance is small even at the limits of the measuring range. The maximum tolerance is 2% relative humidity or ±0.3°C over a wide range. This enables the new SHT25 to achieve significantly better accuracy, especially for temperature measurements.

The SHT25 is fully calibrated and exactly matches the other specifications of the already successful SHT21 version. Among other things, the SHT25 can be reflow-soldered and it has an I2C interface and features outstanding stability along with extremely low power consumption. As with the SHT21, the new version is available on tape & reel.

www.sensirion.com

APACER LEAPS FORWARD WITH THE SMALLEST AND LIGHTEST SSD ON THE MARKET

Apacer Technology's 6-gram SDM 7P/180D-LP (SATA Disk Module 7Pin/180Degree-Low Profile) is one of the smallest SSDs on the market. With a SATA interface, which is only 12% of the size of a conventional 2.5" hard disk, the SSD is 90% lighter.

The products unique hook design along with the innovative concept of ridding of power cables, fully demonstrates the advantages of the shockproof feature and built-in power supply. The design of the SSD includes a unique power circuit on two sides of the connector, which maintains signal integrity and greatly increases product stability. This ensures 100% firm contact with the connector, which eliminates the problem of loose or power cables coming off due to impact or vibration.

Apacer Technology offers one of the most complete product lines which includes 7P/180D-LP as well as 7P/90D and 7P/270D SATA SSDs, with capacities ranging from 512 MB to 8 GB.

www.apacer.com

PARTNERSHIP FOR SUPERSPEED USB 3.0 DEVELOPMENT SOLUTIONS

LeCroy and Evatronix have announced a partnership agreement that aims to aid the faster market adoption of the SuperSpeed USB 3.0 technology by cooperation on mutual product development and USB market investigation. The partnership hopes to bring new added value to SuperSpeed USB 3.0 application developers.

The LeCroy USB 3.0 Test Suite includes the SDA 813Zi-A oscilloscope for physical layer transmitter verification, compliance and debug; the protocol-enabled receiver and transmitter tolerance tester, PeRT3, for receiver testing; the SPARQ Signal Integrity Network Analyzer for S-parameter critical characterization and TDR measurements; and the world's first USB 3.0 protocol analyzer exerciser platform, the Voyager verification system, to address the protocol layer.

The LeCroy PeRT3 is a receiver tester that integrates receiver test with protocol awareness. It provides the ability to automate testing through active control of the device under test. It is also able to easily manage through protocol issues such as SKP symbols which can interrupt testing on competitive products.

www.lecroy.com

NEW FEATURES FOR THE CT ANALYZER

Omicron's CT Analyzer provides fast and comprehensive testing of current transformers for protection and metering applications.

Released in September, the improved CT Analyzer now features additional software functions and new hardware accessories. As a new measurement function for the CT Analyzer, the RemAlyzer allows current transformers to be tested for residual magnetism. Residual magnetism may occur in current transformers due to very high currents or DC offsets during fault conditions. Core saturation effects caused by residual magnetism, may lead to the incorrect operation of protection relays.

The new CT SB2 switch box for the automated testing of multi-ratio CTs is available as a stand-alone unit. This can be attached to the CT Analyzer thus eliminating the need for re-wiring. This provides simple, color-coded, six-channel connection possibilities guaranteeing convenient wiring and avoiding time-consuming and error-prone reconnection.

www.omicron.at

MICROLEASE ADDS POWERFUL TEKTRONIX SPECTRUM ANALYSERS AND OSCILLOSCOPES TO ITS INVENTORY

Microlease has added two new high-performance instruments from Tektronix to its inventory. These instruments are ideal for bench testing and debugging high bandwidth data devices, making them ideal for new product development applications.

The Textronix RSA6120A real-time spectrum and vector analyser is capable of measuring bandwidths up to 20GHz. The integral spectrum processing engine uniquely allows live discovery, triggering, capturing and analysis of transient events, making the instrument ideal for spotting instabilities and other design issues. Applications include RF and radar systems, radio and satellite communications and spectrum management.

The DPO7354 is the high-performance digital phosphor oscilloscope, which provides high-speed 3.5GHz bandwidth with precision TFT displays for accurate real-time signal fidelity. It is ideal for maintaining excellent signal integrity, jitter and timing analysis for sophisticated designs, debugging and compliance testing of serial data streams in the telecoms and data communications applications.

www.microlease.com

ROHS COMPLIANT EMC VENTILATION PANELS

Kemtron has introduced a RoHS compliant aluminium passivation process for its aluminium honeycomb EMC ventilation panels. The process has eliminated the hexavalent chromium which is present in some aluminium passivation processes; the new conversion coating meets the requirements of Mil-C-5541E for corrosion and electrical conductivity.

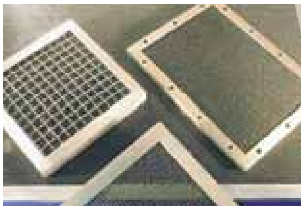

Kemtron has also invested heavily in a new state-of-the-art production facility to make the EMC Honeycomb Vent Panels. Fully programmable CNC machines for the notching and cutting of the frame extrusions and drilling of exact and repeatable holes combined with the latest TIG welding equipment allows Kemtron to offer a fast delivery, competitive range of aluminium vent panels produced to customer designs. This advanced technology also eliminates the need for additional tooling and set-up charges needed with older production techniques.

The standard honeycomb vent panel is constructed from two layers of aluminium honeycomb set at 90° to each other and set in an extruded aluminium frame.

www.kemtron.co.uk

AVX EXPANDS STACKED MLCC FAMILY

AVX has expanded its stacked, surface mount multilayer ceramic capacitor (MLCC) product offering to include the highest capacitance for a given MLCC package. The range extension features 50V and 100V devices with maximum capacitance values of 33uF and 22uF respectively. The advanced capacitor series provides excellent over voltage protection, improves ripple current capability and VC performance compared to other high capacitance MLCCs, while offering low ESR.

Featuring a stress relieving lead frame, the RH Series is ideal for any application requiring board stress relief. Suitable for military and aerospace applications, the RH Series can be used as an input and output filter capacitor in high frequency DC-DC converter applications above 10W, where high volume and low cost is required.

The RH Series is available in RoHS and non-RoHS versions, and come in tape and reel packaging or waffle trays.

The RH Series has a typical lead time of 12 weeks.

www.avx.com

LINEAR HALL-EFFECT CURRENT SENSOR IC

The new ACS711 from Allegro MicroSystems Europe is a Hall-effect linear current sensor IC with a built-in overcurrent fault output that provides economical and precise AC or DC current sensing in audio, communications, white goods and automotive applications operating at voltages up to 100V.

The ACS711 consists of a linear Hall sensor circuit with a copper conduction path located near the surface of the die. Applied current flowing through this copper conduction path generates a magnetic field which is sensed by the integrated Hall IC and converted into a proportional voltage. Device accuracy is optimised through the close proximity of the magnetic signal to the Hall transducer.

The output of the device has a positive slope proportional to the current flow from the positive to the negative input pins. The internal resistance of this conductive path is typically 1.2 milliohms, providing a non-intrusive measurement interface that saves power in applications that require energy efficiency.

www.allegromicro.com

RITTAL'S RIPAC SUBRACKS ALLOW MYRIAD OPTIONS

Rittal's wide range of subracks, all branded under the Ripac banner, provide users with multiple options for housing several printed circuit boards or plug-in modules in a 19" rack environment.

Ranging from the Ripac EASY with simple, non-EMC construction and ultra-quick assembly to the highly competitive Ripac Vario EMC for more sophisticated applications, the whole range shares common accessories, such as guide rails and divider kits for use where different sized PCBs are to be accommodated.

Other parts of the range provide support for heavy loads (Ripac Solid), or are designed for simple mounting on DIN rails for a few boards (Ripac Compact). The backbone of the range, Ripac Vario, may be upgraded to an EMC solution following assembly if it is found necessary.

In addition to catalogues and an Internet based configurator, Rittal offer personal assistance with subrack and case design and backplane selection, through their team of 20 area managers and market specialists.

www.rittal.co.uk

Elektra 2010
European Electronics Industry Awards
FINALIST

MOUSER NOMINATED FOR PRESTIGIOUS ELEKTRA EUROPEAN DISTRIBUTOR OF THE YEAR

Mouser Electronics was nominated as a Finalist for Elektra's 2010 Distributor of the Year Award for Europe.

An annual highpoint of the electronics industry, the Elektra 2010 European Electronics Industry Awards, selected by an independent panel of judges, recognize the achievements of individuals and companies across Europe. They promote the best practice in key areas, including innovation, sales growth and employee motivation.

"It is very exciting for us to be nominated as a finalist for Elektra Distributor of the Year in Europe," said Mark Burr-Lonnon, Mouser VP of EMEA and APAC Business. "Mouser opened our first European office just two years ago, and already we've become one of the top distributors in EMEA among design engineers.''

"Our ultimate goal is to help design engineers across the globe easily find the latest components and leading technologies to get their products to market faster,'' he added.

www.mouser.com

NEW NEXT GENERATION AVIONICS CONNECTOR INSERTS FROM ITT ICS

ITT Interconnect Solutions, has announced a new Applications Note detailing the use of its ARINC 600 next generation connector inserts for aircraft flight control avionics. Increased data transmission rates are required by the latest data communications and aircraft landing systems and ITT ICS engineers have met this challenge by designing a new series of robust, compact inserts to which allow signal, power, Ethernet and fibre optic data transmission functions to be combined into a single interconnect.

These weight and space-saving inserts suit many aerospace applications, including instrument landing systems, GPS landing systems, flight navigation systems, avionic common data network systems, integrated surveillance systems and backbone Ethernet network modules.

Three new interconnect inserts have been developed – 30Q2, 13Q2 and 17Q2 – which can all also be combined with existing signal, power and quadrax inserts to develop an infinite combination of connector layouts which will meet future bandwidth requirements.

www.ittcannon.com

eMOBILITY CHARGING CONNECTORS AVAILABLE FROM FOREMOST

Foremost Electronics announces the introduction into the UK of the eMobility range of electric vehicle charging connectors manufactured by FCT Electronic GmbH.

A leading manufacturer of high reliability connectors, FCT has developed this new range of charging connectors for the worldwide net integration of electric vehicles. Increasingly powerful electrically-charged vehicles are being developed by car manufacturers worldwide as solutions are being found for the technical challenges of vehicle cruising range and charging cycles.

After a development time of just three months, the innovative eMobility charging connector was field tested in Israel where complete integration of an electric vehicle network architecture on a national level is planned. The project is then expected to be rolled out in further countries such as Denmark and Austria.

Standards in the automotive industry are particularly stringent as not only climate conditions extreme but even more intensive operational conditions, such as the effects of salt and sand, must be provided for.

www.4most.co.uk

LABSPHERE LAUNCHES HIGH SPEED LED CHARACTERIZATION SPECTROMETERS

Designed for a full range of LED characterization measurements, Labsphere has introduced the CDS-5400 and CDS-9800 High Speed LED Spectrometers. Both models offer reliability, speed and accuracy with a choice of spectral range to suit specification application needs.

The CDS spectrometers, when integrated into Labsphere's systems, measure critical spectral characteristics of LEDs including flux; intensity; chromaticity coordinates; dominant, peak and centroid wavelengths; colour temperature and rendering properties; and purity. To capture and organize data, DLL drivers are available to connect the spectrometers to proprietary QA, calibration and production software.

With a spectral range of 305-930nm, the CDS-5400 is well suited for production line testing of high brightness LEDs. With a 2ms integration time, the CDS-5400 delivers the high speed required by these environments. For more high precision applications including fixed quantity UV and quantum efficiency measurement, the CDS-9800 has a wide dynamic range and four models covering the spectral range of 240-1100nm.

www.labsphere.com

JOINTLY DEVELOPED SOFTWARE FOR **CPU VIRTUALIZATION TECHNOLOGY**

Semiconductor vendor Renesas Electronics and operating systems supplier SYSGO are jointly developing basic software supporting CPU virtualisation technology suitable for real-time control applications.

Through the collaboration, Renesas Electronics will develop added functions necessary for the efficient operation of virtualisation software enabling high-speed real-time control and improving the usability of the software development environment, incorporating these functions into microcontrollers with V850 CPU core.

SYSGO will port to Renesas Electronics's V850 core its PikeOS hybrid OS, which enables multiple OSes to run simultaneously on a single CPU, providing virtualisation support. SYSGO will assess PikeOS in actual automotive and other applications, and the feedback of their evaluation results will be used to optimize further the specifications. In addition to complying with functional safety standards, such as DO-178B (Note 1) and EN50128 (Note 2), the basic software to be developed will include support for the envisioned ISO 26262 functional safety standard and provide security functionality such as support for MILS (Note 3) and EAL (Note 4).

Our panel of commentators says the following on this development:

PROFESSOR DR DOGAN IBRAHIM, THE NEAR EAST UNIVERSITY IN NICOSIA, CYPRUS: V850 is a 32-bit CPU core designed to support single-instruction-multiple-data (SIMD), suitable for high performance. Most of the current signal-processing architectures include external DSPs with low-speed memories and the response of such architectures is limited. The architecture of V850 combines the control performance of its CPU core with the high-speed signal-processing performance and special enhanced signal processing functions, making it an ideal processor for real-time control applications.

PikeOS is a microkernel-based real-time operating system developed for multiple CPU virtualisations, and targeted for safety and security critical applications, supporting diverse hardware platforms. The collaboration between Renesas Electronics and SYSGO will certainly result in the development of highly flexible and high-performance real-time platforms, currently needed for the growing embedded automotive and other control based applications.

BARRY MCKEOWN, RF AND MICROWAVE ENGINEER IN THE DEFENCE INDUSTRY, AND DIRECTOR OF DATOD LTD, UK: The chemists call it a catalyst: it both initiates and controls a reaction's rate. In real-time systems' engineering we are still searching for catalysts. Since circa 2006 IT servers have been able to attain 24/7/52 operation via virtualisation. If this V850 initiative attains for microcontrollers and similar programs for FPGAs then systems engineering will undergo another profound change in design methodology. Virtualisation shall enable greater flexibility in real-time smart grid systems and distributed control of networked infrastructure support and maintenance. But I suspect that the virtualisation process is far away from attaining the state of being a catalyst.

MAURIZIO DI PAOLO EMILIO, TELECOMMUNICATIONS ENGINEER, INFN – LABORATORI NAZIONALI DEL GRAN SASSO, ITALY: Virtualisation helps engineers better utilize their available processing hardware to build more efficient systems.

It is important to note that virtualisation is not being used only in the engineering domain. Many information technology companies have used virtualisation to consolidate large groups of servers at a savings that can reach millions of dollars.

With virtualisation it is possible to take advantage of the capabilities offered by different operating systems, save hardware cost and footprint, and make use of multicore processors. The prevalence of multicore processors on the computing scene is now a fact of life, and OEMs are experimenting with ways to partition their applications on different processor cores.

So, virtualisation is also one way to create secure machines. This reduces the need for multiple physical computers that operate at different security levels but are not fully utilized.

HAFIDH MECHERGUI, ASSOCIATE PROFESSOR IN ELECTRICAL ENGINEERING AT THE UNIVERSITY OF TUNISIA: In competition, drawn by innovation and fast products renewal, the co-operation between the companies represents one of the principal organisational levers which are mobilized by the actors in the purpose to have a competitive advantage.

As a proof of this, many collaboration efforts exist in various sectors of the industry. The increasing complexity a product may require and, indeed, the integration of diversified knowledge fields leads to the combination of different technologies in the course of development. Hence we have the co-operation between Renesas Electronics, the supplier of the advanced semiconductors solutions, and SYSGO- the developer of operating software. This co-operation idea allows the realisation of a microcontroller working in real-time and the development of virtualisation software.

The MCU by Renesas Electronics and SYSGO allows a complete management of the sessions and the physical virtual environments which ensure increasing manageability, security, flexibility and virtualisation technology in hardware.

The microcontroller V850 is a sophisticated electronic product, characterised by real time, responsiveness and low power consumption. The V850 is already used in a wide range of applications.

Finally, we can say that one of the principal ways to gain a competitive advantage is to through collaboration i.e. to innovate one's needs to cooperate.

If you'd like to comment on this subject or want to become a member of our panel, please write to the Editor at Svetlana.josifovska@stjohnpatrick.com